ACS OMEGA

http://pubs.acs.org/journal/acsodf

Article

Effects of Polystyrene Microplastics on Human Kidney and Liver Cell Morphology, Cellular Proliferation, and Metabolism

Kerestin E. Goodman, Timothy Hua, and Qing-Xiang Amy Sang*

Cite This: *ACS Omega* 2022, 7, 34136−34153

Read Online

ACCESS | Metrics & More | Article Recommendations | Supporting Information

ABSTRACT: Microplastics have gained much attention due to their prevalence and abundance in our everyday lives. They have been detected in household items such as sugar, salt, honey, seafood, tap water, water bottles, and food items wrapped in plastic. Once ingested, these tiny particles can travel to internal organs such as the kidney and liver and cause adverse effects on the cellular level. Here, human embryonic kidney (HEK 293) cells and human hepatocellular (Hep G2) liver cells were used to examine the potential toxicological effects of 1 μm polystyrene microplastics (PS-MPs). Exposing cells to PS-MPs caused a major reduction in cellular proliferation but no significant decrease in cell viability as determined by the trypan blue assay in both cell lines. Cell viability remained at least 94% for both cell lines even at the highest concentration of 100 μg/mL of PS-MPs. Phase-contrast imaging of both kidney and liver cells exposed to PS-MPs at 72 h showed significant morphological changes and uptake of PS-MP particles. Confocal fluorescent microscopy confirmed the uptake of 1 μm PS-MPs at 72 h for both cell lines. Additionally, flow cytometry experiments verified that more than 70% of cells internalized 1 μm PS-MPs after 48 h of exposure for both kidney and liver cells. Reactive oxygen species (ROS) studies revealed kidney and liver cells exposed to PS-MPs had increased levels of ROS at each concentration and for every time point tested. Furthermore, quantitative reverse transcription polymerase chain reaction (qRT-PCR) analysis at 24 and 72 h revealed that both HEK 293 and Hep G2 cells exposed to PS-MPs lowered the gene expression levels of the glycolytic enzyme, *glyceraldehyde-3-phosphate dehydrogenase* (*GAPDH*), and antioxidant enzymes *superoxide dismutase 2* (*SOD2*) and *catalase* (*CAT*), thus reducing the potential of SOD2 and CAT to detoxify ROS. These adverse effects of PS-MPs on human kidney and liver cells suggest that ingesting microplastics may lead to toxicological problems on cell metabolism and cell−cell interactions. Because exposing human kidney and liver cells to microplastics results in morphological, metabolic, proliferative changes and cellular stress, these results indicate the potential undesirable effects of microplastics on human health.

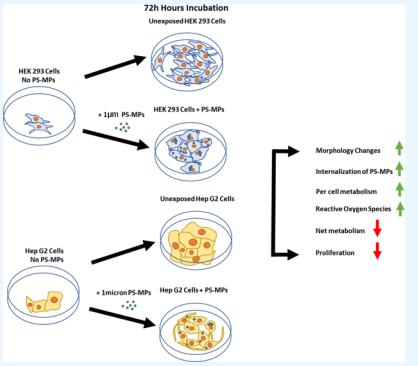

INTRODUCTION

Plastic pollution is one of the most dynamic issues affecting climate, environment, and human health. As more single-use plastics are being produced and the global demand for these plastics increases, our ability to deal with the inevitable plastic waste becomes more problematic each year. The visibility of plastic waste is increasing as more plastics are polluting oceans, rivers, lakes, and air.[1−3] Multiple aspects of human lives are affected by plastics. The global production of plastic reached 368 million tons in 2019, and single-use plastics make up approximately 50% of all the plastics produced.[4,5] Although single-use plastics make up the majority of plastic waste, less than 14% of plastics found in municipal solid waste gets recycled each year.[6] Bags, water bottles, cutlery, and straws are used in homes, businesses, theme parks, schools, and other places people live, visit, and work each day. These single-use plastics and other plastic waste are sent to landfills, incinerated, and often improperly disposed of, contributing to even more plastic waste in the environment.

Plastics can take many years to decompose, so they accumulate and begin to break down once discarded. The breakdown of plastics occurs through radiation from the sun, mechanical forces from waves, and other physical and thermal processes.[7] The degradation of these plastics leads to the generation of even smaller plastics, called microplastics. Microplastics (<5 mm in size) significantly impact today's society with the increasing discovery that they are essentially everywhere. Microplastics can be transported to multiple places through wind, dust, atmospheric fallout, snow, and various bodies of water (i.e., rivers, lakes, and oceans).[8−13] Microplastics have been found in forests, cities, and even the most remote places such as the Swiss Alps and the glaciers of the Tibetan Plateau.[14−17] Microplastics are ubiquitous in the environment, and more studies have documented microplastics in human consumables raising even more concern for human health and exposure.

Received: June 2, 2022
Accepted: September 5, 2022
Published: September 19, 2022

Ingestion of microplastics is one of the major routes of human exposure.[18] It is estimated that Americans consume 39,000−52,000 microplastics annually in food and beverages.[19] Researchers reported that microplastics could enter the food chain through plastic packaged goods (such as water bottles, processed foods, meat, etc.), ingestion of microplastics via seafood and groundwater contamination.[19] Recent reports have documented microplastics in human food, food-related products, and the environment, raising more concern for human health. Researchers have detected varying levels of microplastics in various food items. A recent study collected honey samples from Europe and reported an average of 9 fragments/kg of microplastics in honey and an average of 32 fragments/kg of microplastics in sugar.[20] For salt, researchers reported an average of 9.77 item/kg of microplastics in a study carried out in Taiwan, an average of 32 item/kg in a study carried out in the U.S., an average of 46 item/kg in an Australian study, and an average of 58 item/kg in a Croatian study.[21,22] These studies show that the difference in microplastics found in salt varies from region to region. Although the daily intake per person can vary, microplastics can be ingested by salt intake.

In addition to food items, beverages and beverage products provide another way humans could consume microplastics. A recent study reported that a person brewing a tea bag at 95 °C could release over 11 billion microplastics into a single cup. Authors predicted that up to 4.6 tons of microplastics could be released from tea bags during the steeping process.[23] Additional studies found an average of 12−109 fragments/L in German beer, an average of 182−496 fragments/L in Ecuadorian industrial beer, and 50−920 fragments/L in Ecuadorian craft beer.[24,25] Other studies reported that microplastics were found in water. A study reported 3.4−6.3 $\times 10^2$ item/L in drinking water in the Czech Republic, while another study reported 9.3 $\times 10^2$ item/L in drinking water from China.[26,27] For tap water, a study reported 1.8 item/L in Ireland, 7.8 item/L in Cuba, and 9.2 item/L in the U.S.[28] Also, sampled bottled water reported 2.6 $\times 10^3$ item/L in Germany, Italy reported 5.4 $\times 10^7$ item/L, and Thailand reported 4.7 $\times 10^2$ item/L.[29−31] Given that the consumption of water is 1.4 L/day for an adult, it is very likely that drinking water is the most pervasive way that humans ingest microplastics.[32]

Another way that humans can consume microplastics is through the consumption of seafood. In 2016, the United Nations reported that of the 800 marine species that were contaminated with microplastics, 220 of them ingested microplastics from nature.[33,34] In 2011, the estimated global demand for seafood intended for humans to eat was 143.8 million tons, and the amount of seafood that humans consume globally per capita is over 20 kg/year.[35,36] In the United States, the amount of seafood consumed per person increased from 16.1 pounds in 2018 to 19.2 pounds in 2019.[37,38] Furthermore, it was reported in 2016 that over 90% of imported seafood came from locations where there was a significant amount of plastic pollution.[33] Different studies have reported microplastics in seafood intended for human consumption. A Singapore study that analyzed microplastics in commercial shrimp reported an average of 13.4−7050 items, and another study that sampled shrimp in the Arabian sea reported a microplastic average of 1220 items.[39,40] For studies carried out on mussels, researchers found an average of 1.53 items/g in green mussels sold in Thailand, an average of 0.9−4.6 items/g in mussels found on the coastlines in China, and an average of 1.4 items/g of supermarket-bought mussels in the United Kingdom.[41−43] Another study compared the amount of microplastic in fish sold for human consumption. Fish from Fiji had 0.86 pieces/fish, almost two times lower than the average of 1.58 pieces per fish reported in an Australian study.[44] These studies show that microplastics are pervasive even in seafood. Thus, human consumption of microplastics via seafood is likely.

Studies have shown that ingestion of microplastics in marine organisms can cause oxidative stress, inflammatory responses, decreased fertility, decreased eating habits, and other toxicological effects.[45−50] With marine organisms being a prominent food source for humans, it is no surprise that the first microplastic studies documenting toxicological effects due to microplastic exposure were carried out on these organisms. These studies have been carried out on fish, oysters, shrimp, mussels, and other marine organisms to better understand the extent and impact microplastics have on marine wildlife and their potential risks to human health. Other studies noted that microplastics, once ingested, can accumulate in certain organs in marine organisms. The liver and kidney are vital in ridding systems of ingested toxins. However, prolonged accumulation can lead to latent health risks. Several studies were carried out to study the translocation and toxicological effects of microplastics in marine organisms after ingestion. In a study carried out on juvenile jacopever (a carnivorous fish), an accumulation of polystyrene microplastics was found in the liver and caused significant damage to the liver, induced a stress response, and altered metabolism in the liver.[51] The researchers also noted that microplastics reduced growth in the jacopever.[46,51] In a study carried out on juvenile crabs, researchers noted an accumulation of microplastics in the liver that caused oxidative stress and an inflammatory response.[52] Furthermore, studies have shown that microplastic accumulation in crabs inhibited growth and that microplastics accumulated in the kidneys of mackerel and scallops.[52−54] Although research and studies have been carried out on marine organisms about the effects of microplastics, there is still little known about their impact on human health. These studies showing that microplastics can travel to the liver and kidneys further emphasized the potential dangers of microplastic ingestion and the need for further research to assess the potential health risks in humans.

Ingestion is a major way that microplastics can enter the human body. Once ingested, microplastics can enter the circulatory system, where they can be translocated to the liver and kidney, two vital organs responsible for ridding the body of toxins. Many studies reporting microplastics entering the body through ingestion have studied the effects of microplastics on colon and intestinal cells.[55−57] However, information about the effects of microplastics on kidney and liver cells is limited.[58,59] Understanding the effects of microplastics on human kidney and liver cells is of the utmost importance to better understand the potential risks to human health. This study was conducted using a human kidney cell line and a human liver cell line to simultaneously study the effects of microplastics in vitro. Microplastics at 1 μm in size were identified in drinking water, bottled water, seafood, honey, and other human consumables, which provide evidence of a realistic way these tiny plastics can be ingested by humans; thus, we used this particle size for our current study.[32,60,61] Furthermore, 1 μm polystyrene microplastic (PS-MP) particles were found in the environment and are relevant to human exposure.[62−66] Therefore, to explore the

https://doi.org/10.1021/acsomega.2c03453
ACS Omega 2022, 7, 34136−34153

effects of microplastics on human kidney and liver cells, the human embryonic kidney 293 (HEK 293) cell line and the human hepatocellular carcinoma (Hep G2) cell lines were utilized to investigate the effect of microplastics. Both cell lines have previously been employed in toxicological studies.[67−73]

Our current study shows that, when exposed to microplastics, both HEK 293 and Hep G2 cells showed a significant decrease in cell proliferation but no significant changes in viability. After 72 h of exposure, the cell population uptook the microplastic particles as high as 95% in HEK 293 cells and 74% in Hep G2 cells. These particles surrounded the nucleus and caused significant metabolic changes. The net mitochondrial reductase activities were significantly reduced, but the activities per cell were significantly increased when exposed to 100 μg/mL. Additionally, reactive oxygen species (ROS) levels in both HEK 293 and Hep G2 cells were found to increase for PS-MP-exposed cells for all concentrations tested and at each time point observed. Furthermore, quantitative reverse transcription polymerase chain reaction (qRT-PCR) analysis revealed that, upon exposure to PS-MPs, both HEK 293 and Hep G2 cells lowered glycolytic enzyme gene expression and reduced the ability of antioxidant enzymes to cleanse ROS in both cell lines. Our study elucidates the adverse effects that microplastics have on cellular morphology, proliferation, stress, metabolism, and internalization in both cell lines.

MATERIALS AND METHODS

Microspheres. The plain and the green-fluorescent polystyrene microspheres (PS-MPs) of size 1 μm were purchased from Degradex (Phosphorex). The size of the particles was provided by the company (Supporting Information, Table S1). In addition, one of our recent publications also further characterized the plain particles using Fourier-transform infrared spectroscopy for the polystyrene chemical bonds and using dynamic light scattering for particle degradation.[74]

Cell Culture and Microplastic Treatment. Human embryonic kidney 293 cells (HEK 293; ATCC CRL-1573) and human hepatocellular carcinoma cells (Hep G2 or HEPG2; ATCC HB-8065) were cultured in Dulbecco's modified Eagle's medium (DMEM; Sigma-Aldrich) supplemented with 10% fetal bovine serum (FBS; Atlanta Biologicals), penicillin, streptomycin, and L-glutamine (Sigma-Aldrich) at 37 °C under 5% CO_2. The cell density per well was 6.4×10^4 cells for 6-well plates and 2.5×10^4 cells for 96-well plates. The cells were passaged when they reached 80% confluence using trypsin (Corning). After plating the cells for 12 h, they were treated with PS-MPs at various concentrations.

Phase Contrast Microscopy for Live Cell Imaging. HEK 293 and Hep G2 cells were plated in six-well plates for 12 h before being treated with 5 μg/mL PS-MPs. The untreated cells were used as a control. At 24, 48, and 72 h, live-cell imaging was carried out using an Olympus OM-1 phase-contrast microscope and the Olympus QColor 3 imaging system at the FSU Institute of Molecular Biophysics Protein Expression Facility. The images were taken at either 100× or 400× magnifications and analyzed using ImageJ (NIH).

Metabolic Assay. To measure changes in cellular metabolic activity, we used the MTT (3-(4,5-dimethylthiazol-2-yl)-2,5-diphenyl tetrazolium bromide) assay.[75,76] The mitochondrial NAD(P)H-dependent oxidoreductase enzymes/dehydrogenases reduce the yellow MTT to purple formazan.[75,76] This MTT assay is widely used to detect cellular metabolic activity as an indicator of cell proliferation, viability, and cytotoxicity. After 12 h of replating the HEK 293 kidney cells and Hep G2 liver cells in a 96-well plate, 1 μm PS-MPs were added to the culture at 0.05, 5, 10, 25, 50, 75, and 100 μg/mL concentrations. MTT assay was carried out for 24, 48, and 72 h time points. Briefly, 3-(4,5-dimethylthiazol-2-yl)-2,5-diphenyltetrazolium bromide (MTT) was added, and the cells were incubated for 2 h. Then, sodium dodecyl sulfate (SDS; Sigma-Aldrich) was used to dissolve formazan crystals that gave a purple color. The solution absorbance was read at 570 nm using a SpectraMax iD5 multimode microplate at the Analytical Laboratory at the FSU Department of Biological Science. Both the untreated and treated conditions were repeated three times. The MTT assay was repeated as a triplicate of independent experiments. The reading from the cell-only condition was subtracted from the reading from just the SDS and used as the blank. Also, the microplastic-treated cell's reading was subtracted from the reading of the microplastic-only condition. The untreated condition was used to normalize the readings.

Cell Proliferation Assay and Trypan Blue Dye Exclusion Assay. The cell proliferation assay was carried out by treating the post-12 h replated HEK2 93 and Hep G2 cells in a six-well plate with 100 μg/mL PS-MPs. The cells were harvested using trypsin at 24, 48, and 72 h time points. Once harvested, they were counted using a Neubauer hemocytometer (Electron Microscopy Sciences) under a phase-contrast microscope. Each time point was counted twice with a triplicate independent sampling for the cell proliferation assay to establish a growth curve. For the trypan blue assay, the trypan blue dye (Thermo Fischer) was added to the cell suspension at a 1:4 ratio. Both live and dead cells were counted using the hemocytometer. The clear cells were counted as live cells, and the blue-stained cells were counted as dead cells. This assay was carried out in triplicate as independent experiments.

Confocal Fluorescence Microscopy for Fixed Cell Imaging. After 12 h of replating in six-well plates, HEK 293 and Hep G2 cells were treated with 5 μg/mL 1 μm, green-fluorescent PS-MPs. After 72 h, the media was removed, and cells were washed three times with phosphate-buffered saline (PBS; Thermo Fisher) before being fixed with 10% neutral buffered formalin (VWR). The cells were stained with 4′,6-diamidino-2-phenylindole (DAPI; Biotium) for nuclear staining and the plasma membrane stain wheat germ agglutinin conjugate 594 (WGA-594; Biotium). The images were taken using the Nikon CSU-W1 spinning disk confocal microscope at the Biological Science Imaging Resource at the FSU Department of Biological Science, and they were analyzed using NIS-Elements-Microscope Imaging software.

Flow Cytometry to Determine the PS-MP Uptaking Ability of HEK 293 and Hep G2 Cells. After 12 h of replating in six-well plates, HEK 293 and Hep G2 cells were treated with 5 and 100 μg/mL 1 μm green-fluorescent PS-MPs. The cell's ability to uptake the microplastics at time points of 24, 48, and 72 h was determined using flow cytometry by quantifying the green-fluorescent signals. After harvesting the cells using trypsin, the samples were washed with PBS three times. Then, 1.0×10^6 cells were acquired with BD FACSCanto II flow cytometry (Beckton Dickinson) at the Flow Cytometry Laboratory at the FSU College of Medicine. Cells incubated with Alexa Fluor 488 Goat-Anti Mouse

https://doi.org/10.1021/acsomega.2c03453
ACS Omega 2022, 7, 34136−34153

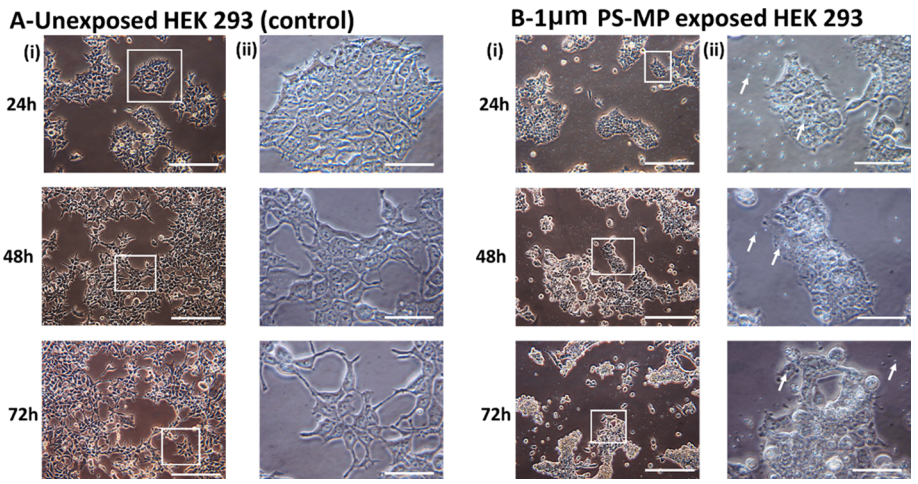

Figure 1. HEK 293 kidney cell phase-contrast images for both (A) unexposed and (B) 1 μm PS-MP exposed cells were taken at 24, 48, and 72 h. After plating, cells were exposed to 5 μg/mL microplastics. The white arrows point to the PS-MPs. At each time point, cells were imaged at (i) 100× and (ii) 400× magnification. Scale bar: 100 μm for (i) and 25 μm for (ii).

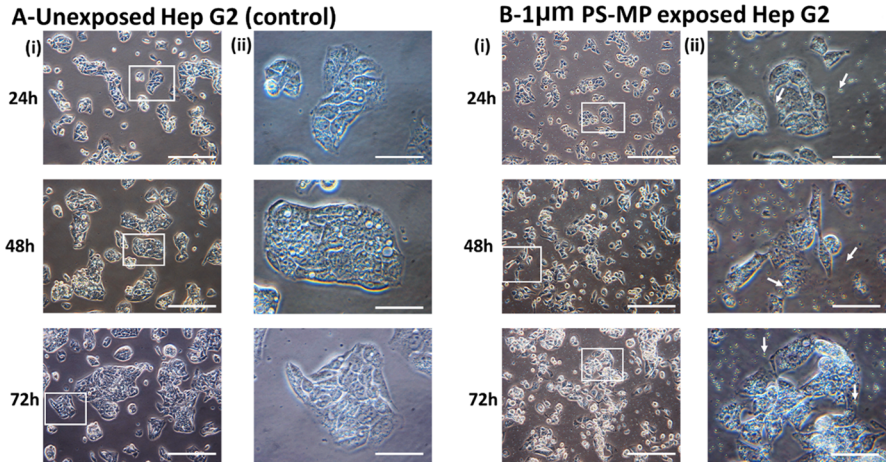

Figure 2. Hep G2 liver cell phase-contrast images for both (A) unexposed and (B) 1 μm PS-MP exposed cells were taken at 24, 48, and 72 h. After plating, cells were exposed to 5 μg/mL microplastics. The white arrows point to the PS-MPs. At each time point, cells were imaged at (i) 100× and (ii) 400× magnification. Scale bar: 100 μm for (i) and 25 μm for (ii).

(Invitrogen) were used as isotype control. The data were analyzed using FlowJo software.

ROS Assay. The Biovision ROS detection assay kit was used to detect real time ROS levels in HEK 293 and Hep G2 live cells. After 12 h of replating in 96-well plates, the ROS label was added to appropriate wells, 1 μm microplastics at concentrations of 5, 50, and 100 μg/mL were added to appropriate wells, and the hydrogen peroxide compound was added to appropriate wells as a positive control. Cells with no ROS label and no microplastics were used as the negative control. ROS levels in live cells were measured at 0, 2, 4, 6, 12, and 24 h time points, and fluorescence was measured using a SpectraMax iD5 multimode microplate at the Analytical Laboratory at the FSU Department of Biological Science.

EdU Cell Proliferation Assay. The Click-It Plus EdU (5-ethynyl-2′-deoxyuridine) imaging kit was used to detect cell proliferation in HEK 293 and Hep G2 fixed cells. Cells were grown for 12 h and plated in six-well plates. The EdU label was then added to cells, 1 μm, green microplastics were added to appropriate wells, and cells were incubated for 24 h. After 24 h, media was removed and cells were fixed using 3.7% formaldehyde in PBS. After fixing, cells were washed twice with 3% BSA in PBS and then permeabilized using 0.5% Triton X-100 in PBS. After permeabilization, cells were washed twice with 3% BSA in PBS. Then, the Click-It Plus reaction cocktail was added to wells incubated for appropriate time and then removed. Following removal of the cocktail, cells were washed once with 3% BSA in PBS. Then, cells were stained with Hoechst 33342 solution and incubated for the appropriate time. After staining with Hoechst 33342, solution was removed from wells, and cells were washed once with PBS. Then, cells were imaged using the Nikon Eclipse Ti Inverted Microscope in the Spectroscopy Lab at FSU Department of Chemistry and Biochemistry.

Quantitative Reverse Transcription Polymerase Chain Reaction (qRT-PCR). After 24 and 72 h, HEK 293 and Hep G2 cells with or without the MP treatment were collected to isolate the total RNA using an E.Z.N.A. Total RNA Kit I (OMEGA Bio-Tek) and purified using an RNA Clean & Concentrator-5 kit (Zymo Research). The reverse transcription experiment was performed using 2 μg of the total RNA, anchored to oligo-dT primers, and Superscript III (Invitrogen) based on the manufacture's protocol. The primer pairs that targeted *beta actin* (*ACTB*, endogenous control),

https://doi.org/10.1021/acsomega.2c03453
ACS Omega 2022, 7, 34136−34153

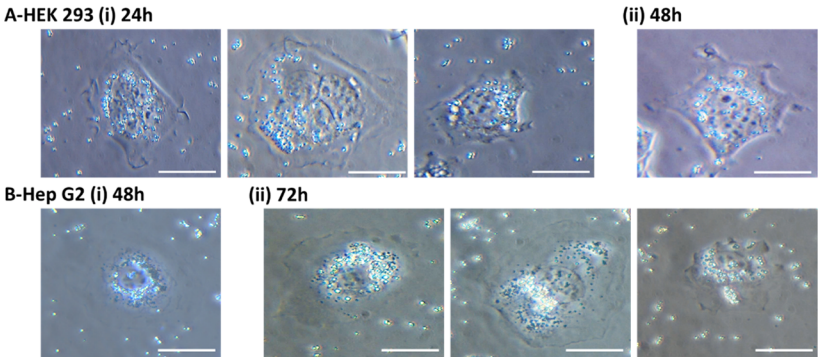

Figure 3. HEK 293 kidney (A) and Hep G2 liver cells (B) show 1 μm PS-MPs surrounding the nucleus at 24 h [A(i)], 48 h [A(ii)] and [B(i)], and 72 h [B(ii)]. These images were taken at 400× magnification. Scale bar: 25 μm.

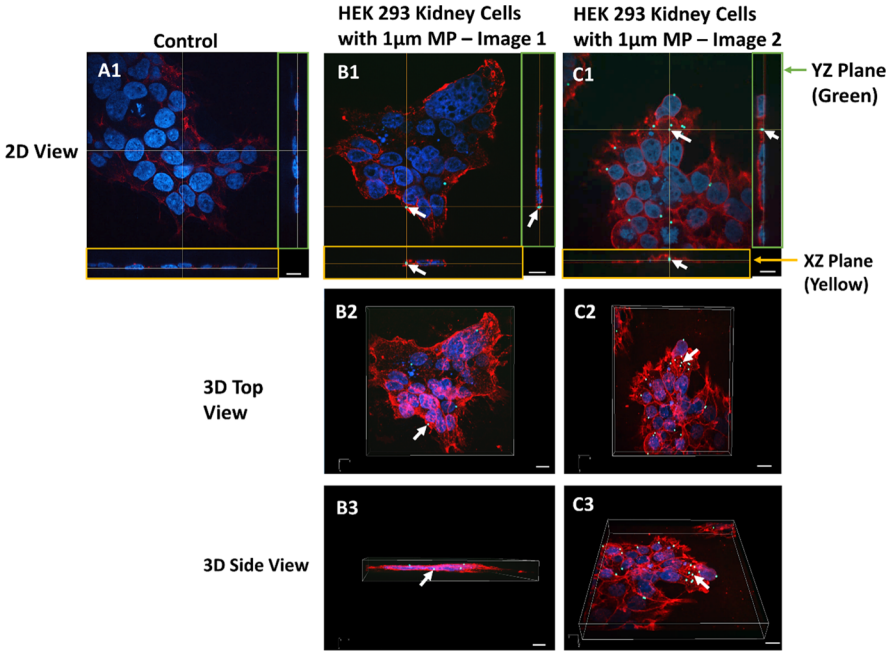

Figure 4. Confocal microscopy images of [A(1)] untreated HEK293 culture and [B(1−3),C(1−3)] 1 μm green-fluorescent polystyrene microplastic particle-treated cultures. HEK 293 kidney cells were exposed to 5 μg/mL 1 μm green-fluorescent PS-MPs for 72 h before fixation. Then, the HEK 293 cells were stained with a wheat germ agglutinin 594 conjugate plasma membrane stain (red) and a nuclear stain DAPI (blue). Panels [A(1)−C(1)] are top-down composites of images in a Z-stack. The internalization of the microplastic is shown in the ortho *YZ* plane {the green box at the right edge of [A(1),B(1),C(1)]} and the *XZ* plane {the yellow box at the bottom of [A(1),B(1),C(1)]}. The white arrows indicate microplastic particles inside the cells. White axes from the particle of interest are drawn to the *XZ* and *YZ* panels on the sides and point out the dimension of the cell that is seen in the top-down view. Panels [B(2),C(2)] show 3-D top view angles of [B(1),C(1)] images, respectively. Panels [B(3),C(3)] show the 3-D side view angles of [B(1),C(1)] images, respectively. These images were taken at 1000× magnification. Scale bar: 10 μm.

GAPDH (glycolysis), *SOD2*, and *CAT* (ROS cleanup) (Supporting Information Table S2) were designed using Primer-BLAST (NIH) and NetPrimers (PREMIER Biosoft). The reaction was carried out using an ABI7500 instrument and SYBRI Green PCR Master Mix (Applied Biosystems). The RT-PCR amplification was 2 min at 50 °C; 10 min at 95 °C; and 40 cycles of 95 °C for 15 s; 55 °C for 30 s; and 68 °C for 30 s. The Ct values were normalized with the expression of *ACTB* before relatively analyzed against the untreated conditions (Figure 12A,B) or the 24 h condition (Figure 12C) using the $2^{-\Delta\Delta C_t}$ method.

Statistical Analysis. Flow cytometry, MTT assay, and RT-PCR were performed as triplicates. The results were represented as [mean ± standard deviation]. When comparing two conditions (Figures 6 and 12C), Student's *t*-test was performed to determine the significance (p-value < 0.05). On the other hand, when comparing more than two conditions (Figures 7−9 and 12A,B), the statistical analysis was performed using analysis of variance (ANOVA), followed by Tukey post hoc test. The significance was determined when the p-value < 0.05.

RESULTS

Morphological Changes and PS-MPs Internalized in HEK 293 Kidney and Hep G2 Liver Cells after Exposure to PS-MPs. PS-MPs of 1 μm size were introduced to the cultures of HEK 293 kidney and Hep G2 liver cells. Phase-contrast microscopy showed morphological differences between exposed and unexposed cultures at 24, 48, and 72 h (Figures 1 and 2). The treated HEK 293 cells altered their

https://doi.org/10.1021/acsomega.2c03453
ACS Omega 2022, 7, 34136−34153

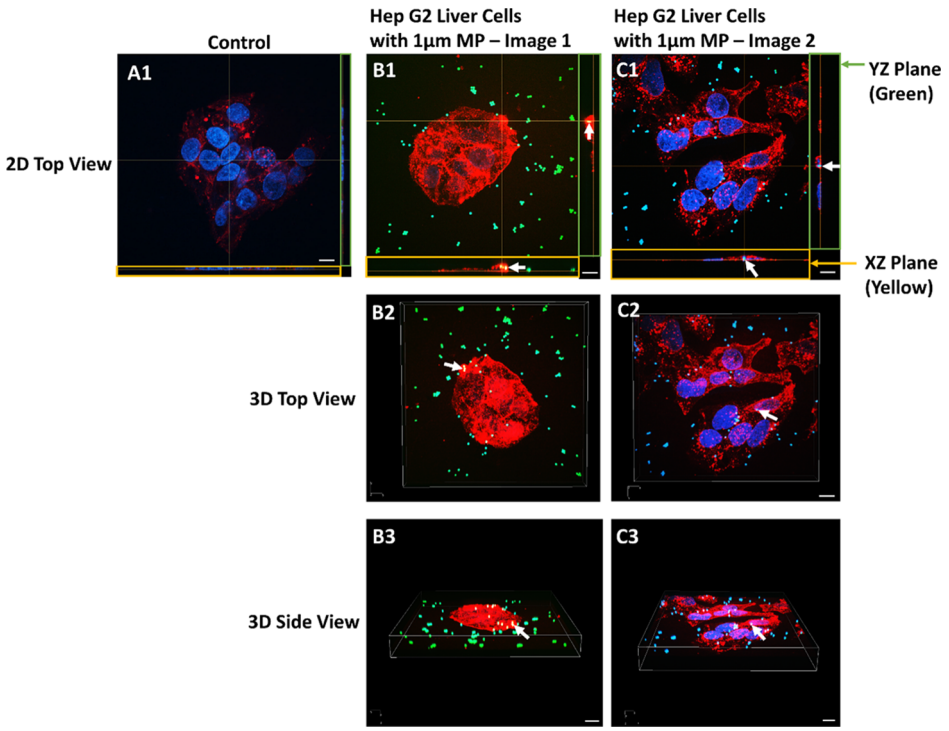

Figure 5. Confocal microscopy images of [A(1)] untreated Hep G2 culture and [B(1−3),C(1−3)] 1 μm green-fluorescent polystyrene microplastic particle-treated cultures. The internalization of the 1 μm microplastics can be visualized in *Z*-axis stacks. Hep G2 cells were exposed to 5 μg/mL 1 μm green-fluorescent PS-MPs for 72 h before fixation. Then, the cells were stained with a wheat germ agglutinin 594 conjugate plasma membrane stain (shown in red) and a nuclear stain DAPI (shown in blue). Panels [A(1)−C(1)] are top-down composites of images in a Z-stack. Internalization of the microplastic is shown in the ortho *YZ* plane {the green-boxed edge right panel of [A(1),B(1),C(1)]} and the *XZ* plane {the yellow-boxed bottom panel of [A(1),B(1),C(1)]}. The white arrows indicate microplastic particles inside the cells. White axes from the particle of interest are drawn to the *XZ* and *YZ* panels on the sides and point out the dimension of the cell that is seen in the top-down view. Panels [B(2),C(2)] show 3-D top view angles of [B(1),C(1)] images, respectively. Panels [B(3),C(3)] show the 3-D side view angles of [B(1),C(1)] images, respectively. These images were taken at 1000× magnification. Scale bar: 10 μm.

morphologies in multiple clusters (Figure 1). Images with a higher magnification focusing on a single-cell cluster are shown in Figure 1A(ii),B(ii).

At 24 h, unexposed HEK 293 kidney cells grew in tight clusters. Along the edges of these clusters, very short pseudopodia projecting from these cells are shown (Figure 1A). The 24 h exposed HEK 293 cells showed similar morphology to 24 h unexposed cells, except 1 μm PS-MPs were observed within the cells (Figure 1B). By 48 h, unexposed cells continued to grow as normal, but exposed cells began to show initial signs of blebbing (Figure 1A,B) As time increased to 72 h, the unexposed culture of HEK 293 kidney cells continued to show large clusters of cells with short pseudopodia projected from the cluster's edges (Figure 1A). However, 72 h exposed HEK 293 cells resulted in severe blebbing in many of the cells, fewer clusters of cells observed and a slight increase in the number of singlets (Figure 1B). This is a stark contrast from the typical morphology demonstrated in unexposed HEK 293 cells. By 72 h of PS-MP treatment, HEK 293 kidney cells had a significant alteration in morphology and a higher uptake of PS-MPs.

At 24 h, the Hep G2 unexposed liver cells grew in tight clusters and are closely packed (Figure 2A). At 24 h, Hep G2 exposed cells still showed similar morphology to unexposed cells, but with the internalization of 1 μm PS-MPs (Figure 2B). At 48 h, 1 μm exposed cells had begun to decluster, while 48 h unexposed cells grew normally (Figure 2A,B). As time increased to 72 h, Hep G2 unexposed cells began to form larger, tightly packed clusters of cells (Figure 2A). However, by 72 h, the exposed culture showed more declustering and more single cells and adapted a morespread-like morphology (Figure 2B). By 72 h, exposed Hep G2 cells had a completely different morphology, had uptaken more PS-MPs, and no longer resembled their unexposed counterparts.

The 1 μm PS-MPs could be observed in both HEK 293 cells and Hep G2 cells as early as 24 h (Figures 1B and 2B). In addition, more microplastic particles were accumulated inside the cells at later time points of 48 and 72 h (Figures 1B and 2B). These particles organized themselves around the nucleus in either a ring-like pattern or in groups in the single cells (Figure 3A,B). Although more particles are internalized in cells over time, particles clustering around the nucleus occur in both early and later time points in both HEK 293 kidney cells and Hep G2 liver cells (Figure 3A,B). This is a similar observation from our previous publication.[62]

Three-Dimensional Z-Stack Images of HEK 293 Kidney and Hep G2 Liver Cells Show the Internalization of 1 μm PS-MPs. HEK 293 kidney and Hep G2 liver cells were exposed to green-fluorescent 1 μm polystyrene microplastics. At 72 h, cells were washed with PBS, fixed, stained, and then imaged using confocal microscopy. The cell membrane was stained red using the wheat germ agglutinin-594 conjugate, and the nucleus was stained blue using DAPI. The particle internalization was shown in z-stack images for both HEK 293 (Figure 4) and Hep G2 (Figure 5).

https://doi.org/10.1021/acsomega.2c03453
ACS Omega 2022, 7, 34136−34153

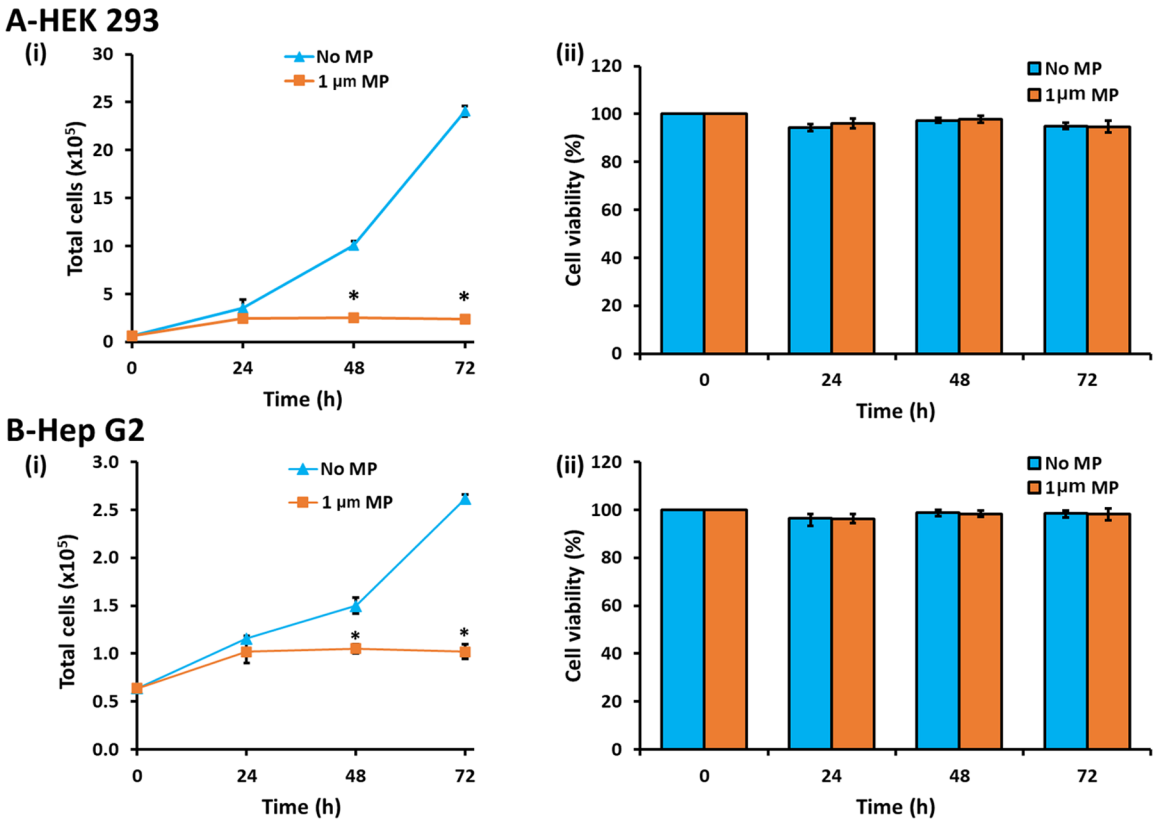

Figure 6. HEK 293 kidney cells (A) and Hep G2 liver cells (B) were characterized for cellular proliferation (i) and cell viability (ii) at time points 0, 24, 48, and 72 h. HEK 293 and Hep G2 cells were exposed to 1 μm polystyrene microplastics (MP) at 100 μg/mL (1 μm MP). The negative control was the unexposed cells (No MP). Student's *t*-test was carried out to determine the significant. *: *p*-value < 0.05.

The ortho *XZ* plane is the yellow box at the bottom side of the 2-D image, and the *YZ* plane is the green box on the right side of the image in the first row of images [Figures 5A(1)−C(1) and 6A(1)−C(1)]. The 3-D *Z*-stack axis of multiple image overlays in B(1),C(1) shows the internalization of the PS-MPs. The green-fluorescent MPs' position relative to the red cell membrane and the blue nucleus can be determined as *XYZ* coordinates. For images B(1) and C(1), *XZ* and *YZ* planes are are vertical sections seen on the paper for the best viewing and are shown at the bottom and right edges of each of the main *XY* images. The intersection of the *XYZ* axes was placed on the microplastic particle, and tracing the axes back to the planes shows the internalized particles with white arrows indicating their position inside the cells. Close-up images showing the internalization of particles shown in A(1)−C(1) in Figures 5 and 6 can be found in Supporting Information, Figures S1−S3 and S5−S7. Each image's separate fluorescent channels are shown in Supporting Information, Figures S4 and S8.

Cellular Proliferation Decreased in Both HEK 293 Kidney and Hep G2 Liver Cells after Exposure to PS-MP. Cellular proliferation was measured using a hemocytometer and a phase-contrast microscope for both HEK 293 kidney and Hep G2 liver cells. HEK 293 kidney cells and Hep G2 liver cells exposed to 1 μm PS-MPs at a 100 μg/mL concentration were counted at time points of 24, 48, and 72 h compared to unexposed cells.

A growth curve was established for both unexposed and exposed HEK 293 kidney cells. The unexposed cells grew as expected from 24 to 72 h, with an initial lag phase, followed by a logarithmic growth phase which is normal for this cell line. Unexposed cells increased more than 3.5-fold from 0 to 24 h and more than 2-fold from 24 to 48 h and from 48 to 72 h. However, microplastic-exposed cells did not follow the same growth trend as unexposed cells, growing much more slowly. Even though it was not statistically significantly different from the unexposed, from 0 to 24 h, microplastic-exposed cells only grew 2.5-fold. Furthermore, from 24 to 48 h, exposed cells barely increased onefold. By 72 h, the final number of cells grown for exposed cells was only approximately 9% of their unexposed counterparts [Figure 6A(i)]. These results reveal that at 48 h, the proliferation of HEK 293 kidney cells was significantly affected by PS-MPs, although they continued to grow after exposure.

For Hep G2 liver cells, a growth curve was also established for both unexposed and exposed cells. The unexposed cells grew normally from 24 to 72 h by exhibiting first a lag phase, followed by a logarithmic growth phase. Unexposed cells increased a little over 1-fold from 0 to 24 h and from 24 to 48 h but did grow over 1.5-fold from 48 to 72 h. From 0 to 72 h, microplastic-exposed cells showed a very consistent onefold growth from 0 to 24 h, 24 to 48 h, and 48 to 72 h. After 48 h, there was a statistically significant difference between the treated and the exposed culture's cell proliferation. The final number of exposed cells grown at 72 h was only approximately 39% of their unexposed counterparts [Figure 6B(i)]. Hep G2 cells exposed to microplastics were inhibited in growth around 48 h. They did not catch up with their unexposed counterparts, and their growth remained stunted at the subsequent time point of 72 h.

Growth curves were established for both unexposed and exposed HEK 293 kidney and Hep G2 liver cells. The result

https://doi.org/10.1021/acsomega.2c03453
ACS Omega 2022, 7, 34136−34153

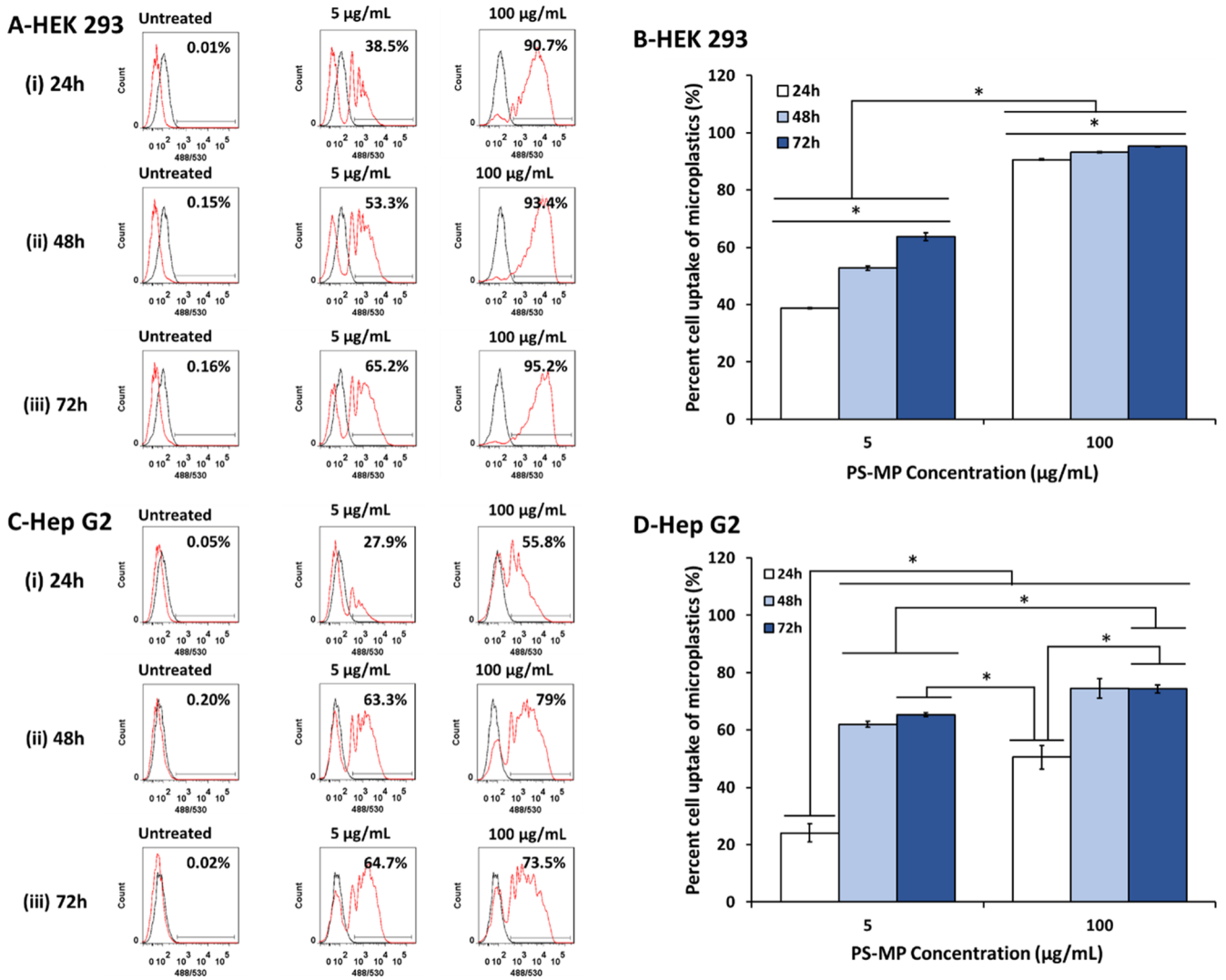

Figure 7. Flow cytometry histograms for trial 1 shown for each condition tested for (A) HEK 293 cells and (B) Hep G2 cells. The bar graph displays the mean percentage of three trials of (C) HEK 293 kidney cells and (D) Hep G2 liver cells that uptook green, fluorescent, 1 μm polystyrene microplastics. Cells were exposed to either 5 μg/mL or 100 μg/mL concentrations of microplastics. At 24, 48, and 72 h, cells were trypsinized, washed with PBS buffer, and then analyzed using flow cytometry. ANOVA followed by Tukey post hoc test was performed to determine the significant. *: p-value < 0.05.

indicated that for both cell lines, exposed cells were unable to keep up with their unexposed counterparts in both growth rate and cell number within the time frame tested after 48 h. 1 μm PS-MPs significantly retarded cell proliferation in both HEK 293 kidney and Hep G2 liver cells.

Cell Viability Remained High in PS-MP-Exposed HEK 293 Kidney and Hep G2 Liver Cells. The trypan blue assay is a dye exclusion assay used to measure the viability of cells. Cells with an intact membrane will not uptake the dye. However, cells with a damaged membrane uptake the dye and appear blue. Unexposed and exposed cells were counted, cells that appeared blue were counted as dead cells, and cells that did not uptake the dye were counted as living cells. Living and dead cells were counted for both exposed and unexposed HEK 293 kidney cells and Hep G2 liver cells. The percentage of live cells for exposed cell cultures of HEK 293 kidney and Hep G2 liver cells remained at least 94% at the highest microplastic concentration of 100 μg/mL tested through 72 h [Figure 6A(ii),B(ii)]. In addition, the statistical significance was not different between the unexposed and the exposed cell viabilities. These results indicate that microplastics did not cause significant cellular death in either HEK 293 kidney or Hep G2 liver cells for each time point tested.

Flow Cytometry of 1 μm Polystyrene Microplastics Shows Uptake in HEK 293 Kidney and Hep G2 Liver Cells. A primary goal of this study was to quantify the percentage of cells that uptook the 1 μm polystyrene microplastics. The cells were grown in six-well plates. Post 12 h, 1 μm green-fluorescent polystyrene microplastics were added to each well. Cell samples were taken at time points of 24, 48, and 72 h, and 5 and 100 μg/mL concentrations were added to designated wells. At each time point, cells were trypsinized, washed with PBS buffer, and then analyzed using flow cytometry (Figure 7). Dot plots for cell population gating and histograms of triplicate for both cell lines for each sample analyzed using flow cytometry are shown in Supporting Information Figures S9−S12. Flow cytometry histograms for Trial 1 are shown below along with the bar graph displaying the mean percentage of HEK 293 kidney cells and Hep G2 liver cells that uptook green, fluorescent, 1 μm polystyrene

https://doi.org/10.1021/acsomega.2c03453
ACS Omega 2022, 7, 34136−34153

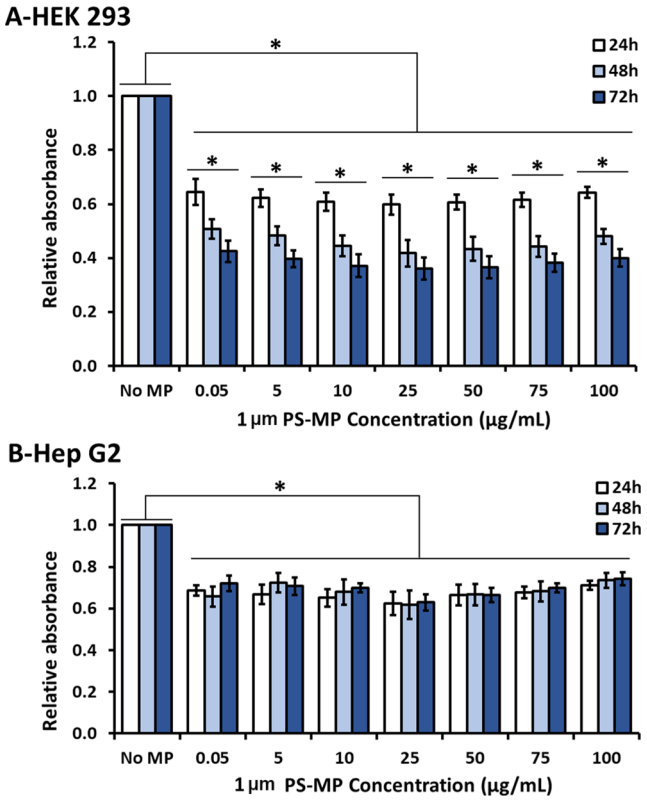

Figure 8. Metabolic activity for HEK 293 kidney and Hep G2 liver cells using MTT. The relative absorbance was analyzed against the no MP controls at each time point. Both cell lines are represented as bar graphs: (A) HEK 293 kidney cells and (B) Hep G2 liver cells. No MP label in the graph represents cells not exposed to microplastics, and 0.05−100 μg/mL are the concentrations cells were exposed to at each time point. MTT absorbance was measured at 570 nm (n = 3). Values for all MP-exposed samples were significantly different from untreated control by ANOVA followed by Tukey post hoc test. *: p-value < 0.05.

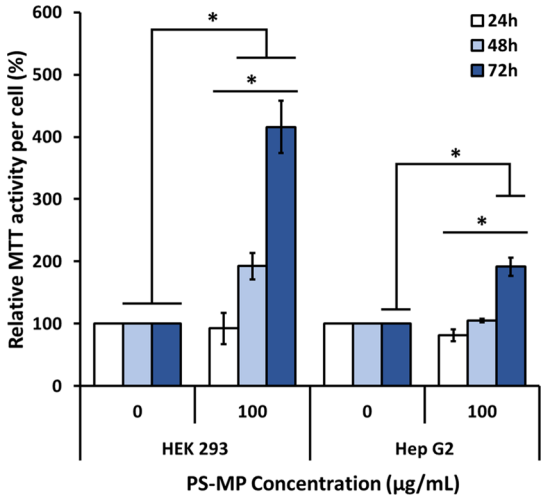

Figure 9. Metabolic activity for HEK 293 and Hep G2 per cell from MTT assay. The MTT readings from Figures 6 and 8 were normalized against the number of live cells and the unexposed activity for both the unexposed and the 100 μg/mL treated cells. The relative MTT activity per cell was analyzed against the no MP controls (0 μg/mL) at each time point. *: p-value < 0.05.

microplastics (Figure 7). All three histograms for the three trials are shown in Supporting Information, Figures S10 and S12.

HEK 293 kidney cells were exposed to 1 μm green-fluorescent polystyrene microplastics for 24, 48, and 72 h at a low concentration of 5 μg/mL and a high concentration of 100 μg/mL. The percentage of cells positive for internalized microplastics was analyzed. At 24 h, for cells exposed to 5 μg/mL, approximately 39% of the cells were positive for microplastics. By 48 h, for cells exposed to 5 μg/mL, that amount increased to approximately 53%, and by 72 h, the percentage of cells that internalized microplastics was approximately 64%. In contrast, HEK 293 kidney cells exposed to the higher concentrations of microplastics had a much higher percentage of cells positive for microplastics at 24 h. At 24 h, cells exposed to the 100 μg/mL concentration had approximately 91% of the cells positive for internalized microplastics, which is 52% higher than the percentage of cells positive at 24 h for the lower concentration 5 μg/mL. At 48 and 72 h, for the higher concentration tested, cells positive for microplastics remained high and consistent with percentages at approximately 93 and 95%, respectively. Although the HEK 293 kidney cells exposed to the lower concentration of microplastics continued to internalize more particles over time, most of the HEK 293 kidney cells exposed to the higher concentration internalized most of the microplastics within 24 h and only slightly uptook more particles at subsequent time points of 48 and 72 h.

Hep G2 liver cells were also exposed to 1 μm polystyrene microplastics for 24, 48, and 72 h at a low concentration of 5 μg/mL and a high concentration of 100 μg/mL. At 24 h, for cells exposed to 5 μg/mL, a mean of 24% of the cells were positive for microplastics. By 48, the mean percentage of cells positive for microplastics increased to a mean of 62% and a mean of 65% by 72 h. In contrast, cells exposed to the 100 μg/mL concentration had a mean of 50% of the cells positive for internalized microplastics. This percentage increased to a mean of 75% at 48 h and went down slightly to 74% by 72 h.

Overall, both cell lines showed differences in the percentage of cells internalizing microplastics over time. HEK 293 kidney cells at a lower concentration of 5 μg/mL had a steady increase in the percentage of cells internalizing microplastics at 24, 48, and 72 h time points. However, the Hep G2 liver cells at the same concentration had an initial increase from 24 to 48 h, but by 72 h, it had only shown a slight increase in the percentage of cells positive for microplastics. For the higher concentration tested, HEK 293 kidney cells showed a high initial percentage of cells positive at 24 h. By 48 and 72 h, the percentage of cells positive for microplastics was slightly higher than the percentage at 24 h. In contrast, at 24 h, the Hep G2 liver cells tested at the same concentration were lower for the percentage of cells positive for microplastics than HEK 293 kidney cells. Furthermore, Hep G2 liver cells positive for microplastics at 48 and 72 h time points remained consistent, showing only a 1% difference. In this study, we found that both concentration and time affected the internalization of microplastics in both HEK 293 kidney and Hep G2 liver cells.

Metabolic Activity Decreased in HEK 293 Kidney and Hep G2 Liver Cells following PS-MP Exposure. To measure metabolic activity, we used the MTT (3-(4,5-dimethylthiazol-2-yl)-2,5-diphenyl tetrazolium bromide) assay, which detects intracellular changes in NADH/NADPH-dependent oxidoreductase/dehydrogenase activ-

https://doi.org/10.1021/acsomega.2c03453
ACS Omega 2022, 7, 34136−34153

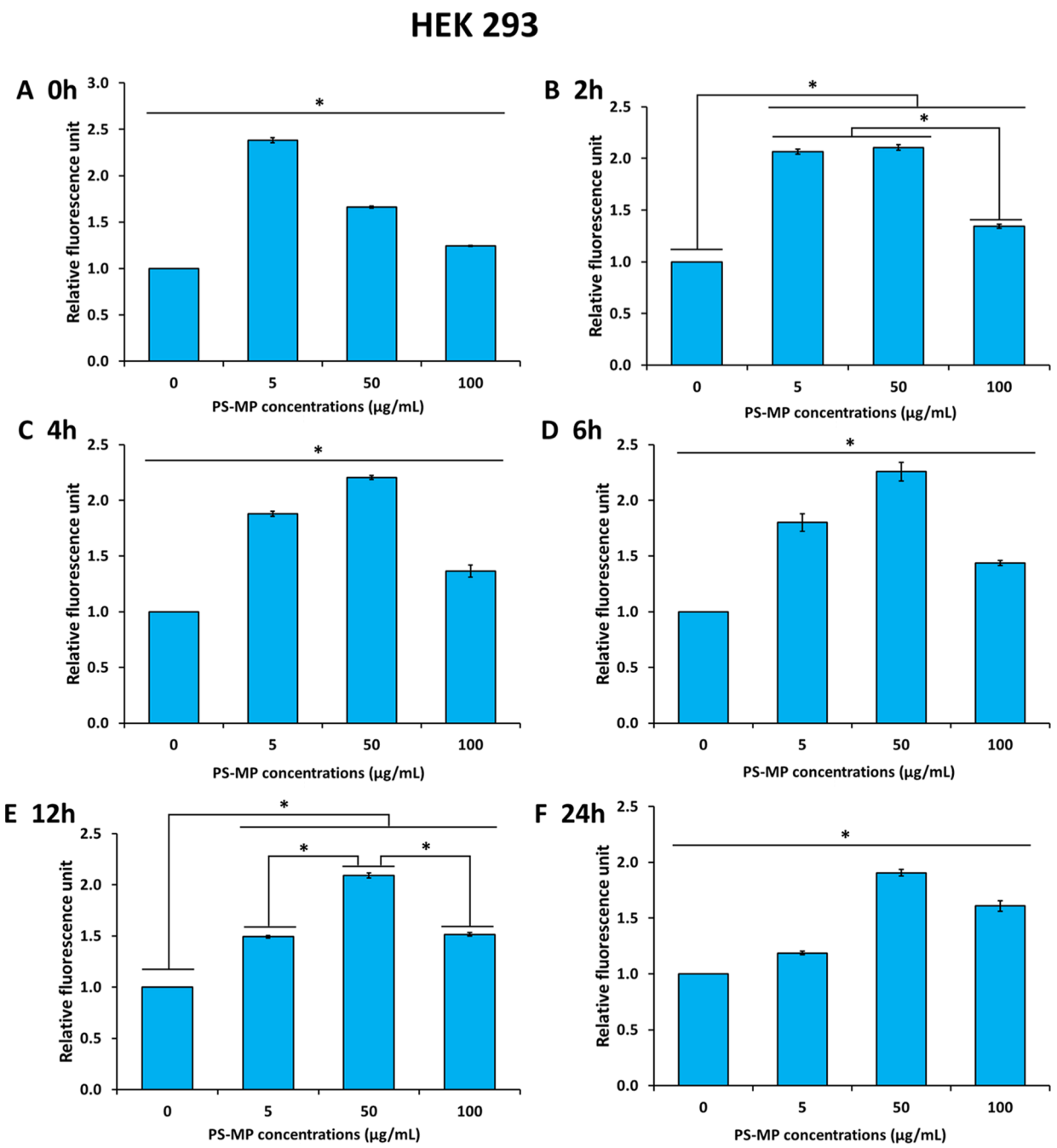

Figure 10. Relative fluorescence units of ROS induced by different concentrations of PS-MPs in HEK 293 cells. The cells were treated with PS-MP before being characterized for the ROS level at different time points including (A) 0, (B) 2, (C) 4, (D) 6, (E) 12, and (F) 24 h. In each time point, the fluorescence units of each concentration were analyzed relatively against the untreated condition of 0 μg/mL, meaning that the relative fluorescence units for 0 μg/mL = 1. ANOVA followed by Tukey post hoc test was performed to determine the significant. *: p-value < 0.05.

ity.[75,76] HEK 293 kidney and Hep G2 liver cells were exposed to 1 μm polystyrene microplastics at concentrations ranging from 0.05 to 100 μg/mL at 24, 48, and 72 h time points and assayed using MTT.

At all time points, HEK 293 exposed cells showed significantly lower absorbance readings from formazan solution as compared to the unexposed control at every condition tested. HEK 293 exposed cells showed approximately a 40% drop in metabolic activity at 24 h, approximately 56% drop by 48 h, and a significant 61% drop by 72 h compared to unexposed cells (Figure 8A). Although there was a slight variation between doses at each time point, these findings indicate that 1 μm PS-MPs can drastically impact the metabolic activity of HEK 293 kidney cells after prolonged exposure.

For Hep G2 exposed cells, all doses caused a similar effect across all time points tested compared to the control. Metabolic activity dropped approximately 30−35% for all time points tested (Figure 8B). Unlike the HEK 293 exposed cells, which showed an initial metabolic decline at 24 h and decreased more over time, the HEP G2 exposed cells showed an initial drop at 24 h. However, the metabolic activity at 48 and 72 h remained consistent with the earliest time point.

https://doi.org/10.1021/acsomega.2c03453
ACS Omega 2022, 7, 34136−34153

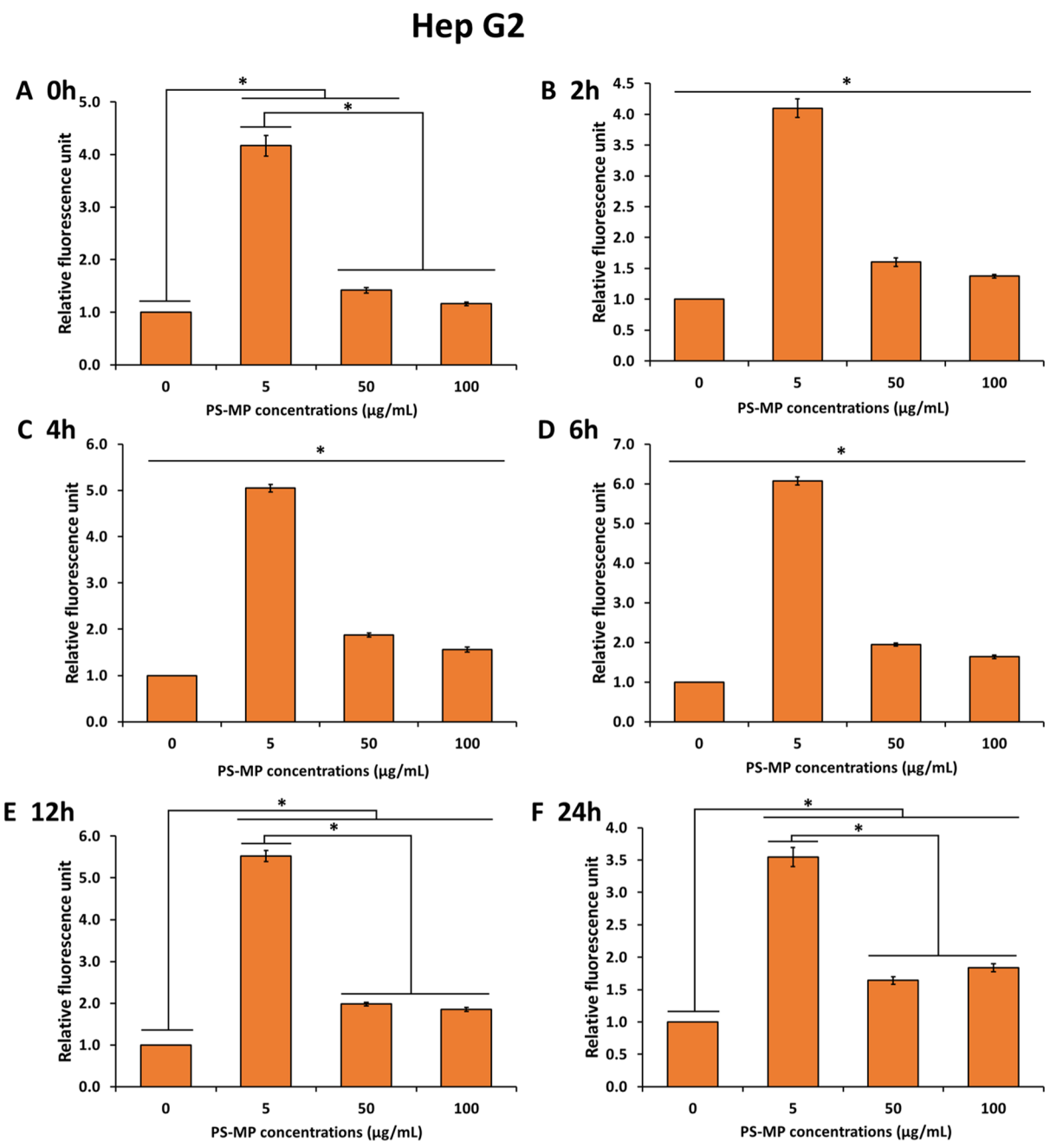

Figure 11. Relative fluorescence units of ROS induced by different concentrations of PS-MPs in Hep G2 cells. The cells were treated with PS-MP before being characterized for the ROS level at different time points including (A) 0, (B) 2, (C) 4, (D) 6, (E) 12, and (F) 24 h. In each time point, the fluorescence units of each concentration were analyzed relatively against the untreated condition of 0 μg/mL, meaning that the relative fluorescence units for 0 μg/mL = 1. ANOVA followed by Tukey post hoc test was performed to determine the significant. *: p-value < 0.05.

Overall cultures of HEK 293 kidney cells and Hep G2 liver cells exposed to 1 μm polystyrene microplastics showed a net effect of lowering levels of metabolic activity as compared to their unexposed counterparts. This net decrease in the metabolic activities was mainly due to PS-MP exposure taken from the cell population as a whole. When you observe per cell metabolic activity, MTT increased in both cell lines (Figure 9). At 72 h, the metabolic activity of both the treated HEK 293 and Hep G2 cells was higher than that of the unexposed cells (416 and 192%, respectively), which is expected when you observe per cell metabolism compared to the entire cell population.

PS-MP Increased ROS Levels in Both HEK 293 and Hep G2 Cell Lines. HEK 293 and Hep G2 cells were grown in 96-well plates. An ROS fluorescent detection label was added to all cells except for the negative control. Cells treated with PS-MPs were exposed to 5, 50, or 100 μg/mL concentrations. ROS levels in live cells were measured at 0, 2, 4, 6, 12, and 24 h time points, and fluorescence was read using a plate reader. For every concentration tested and over the time course of 0−24 h, we observed a steady increase in ROS levels in both HEK 293 cells and Hep G2 cells shown in Supporting Information, Figures S13 and S15. Shown above, we observe how ROS levels at each concentration change with each time point (Figure 10 and 11). In HEK 293, the

https://doi.org/10.1021/acsomega.2c03453
ACS Omega 2022, 7, 34136−34153

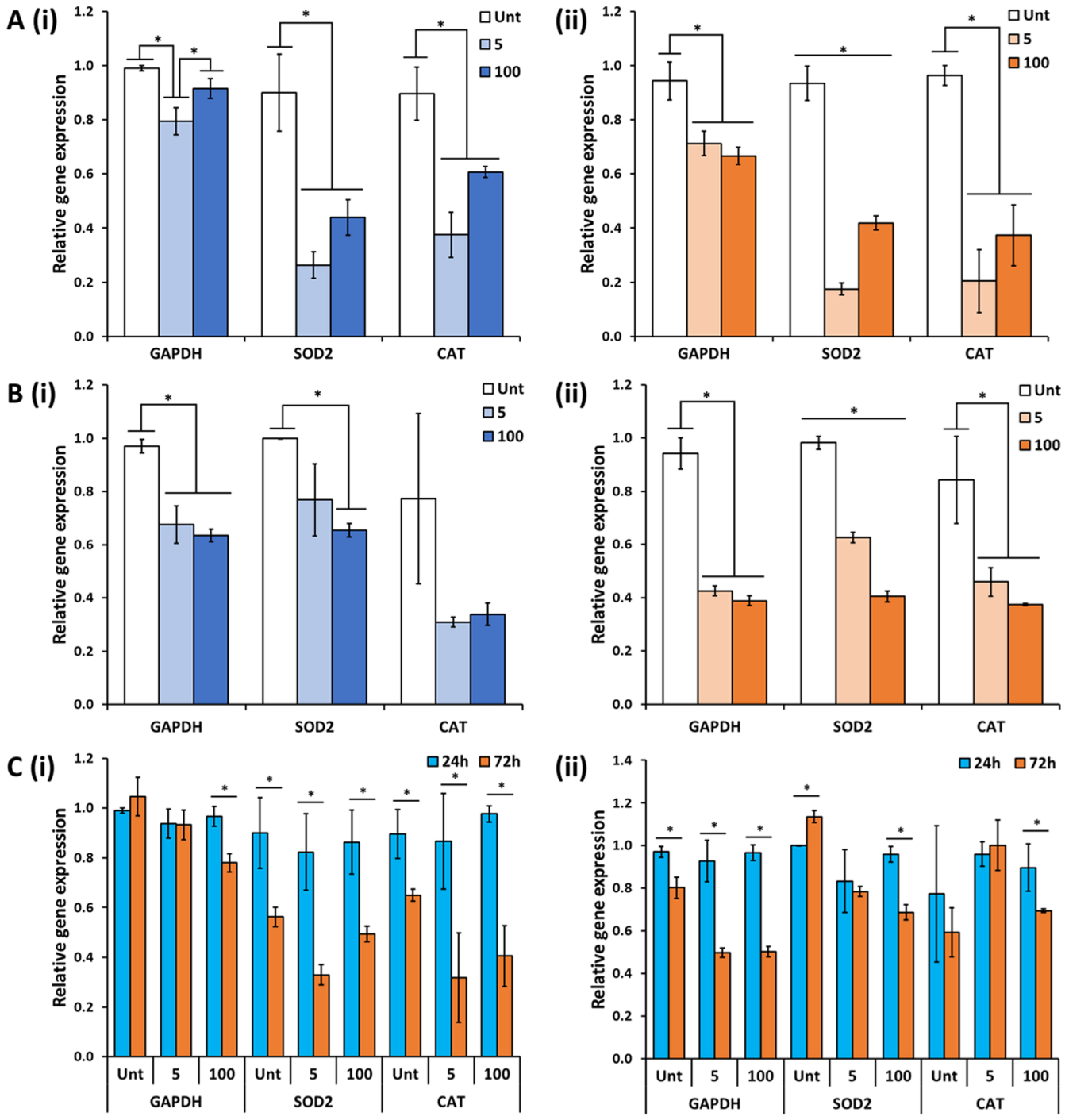

Figure 12. Relative gene expression for glycolysis and ROS cleanup markers for HEK 293 and Hep G2 cells. Both (A) HEK 293 and (B) Hep G2 relative gene expression of the untreated and MP-treated were measured at (i) 24 and (ii) 72 h. The relative gene expression was analyzed against the untreated condition (Unt) for each marker. ANOVA followed by Tukey post hoc test was performed to determine the significant. *: p-value < 0.05. (C) Relative gene expression was reanalyzed to demonstrate the effect of time on each condition for (i) HEK 293 and (ii) Hep G2. *ACTB* was used as an endogenous control. The relative gene expression was analyzed against the 24 h condition for each condition. Student's t-test was carried out to determine the significant. *: p-value < 0.05. CAT: catalase, SOD2: mitochondrial superoxide dismutase 2, GAPDH: glyceraldehyde-3-phosphate dehydrogenase, and ACTB: β-actin.

treatment of PS-MP at 5 and 50 μg/mL induced high levels of ROS as early as 2 h of treatment (Figure 10B). Overtime, there was a slight decrease in ROS induced by the 5 μg/mL compared with 50 μg/mL (Figure 10C−F). Also, 100 μg/mL did not generate as much ROS as 5 and 50 μg/mL for the first 6 h of treatment (Figure 10A−D). However, the ROS induced by 100 μg/mL was comparable to 5 μg/mL after 12 h and even higher after 24 h (Figure 10E,F). Furthermore, at high concentrations (50 and 100 μg/mL), the ROS increased over the first 24 h of treatment (Figure 10B,C). Hydrogen peroxide treatment was used as the positive control, and cells with no MP treatment and no ROS label were used as the negative control (Supporting Information, Figures S14 and S16).

https://doi.org/10.1021/acsomega.2c03453
ACS Omega 2022, 7, 34136−34153

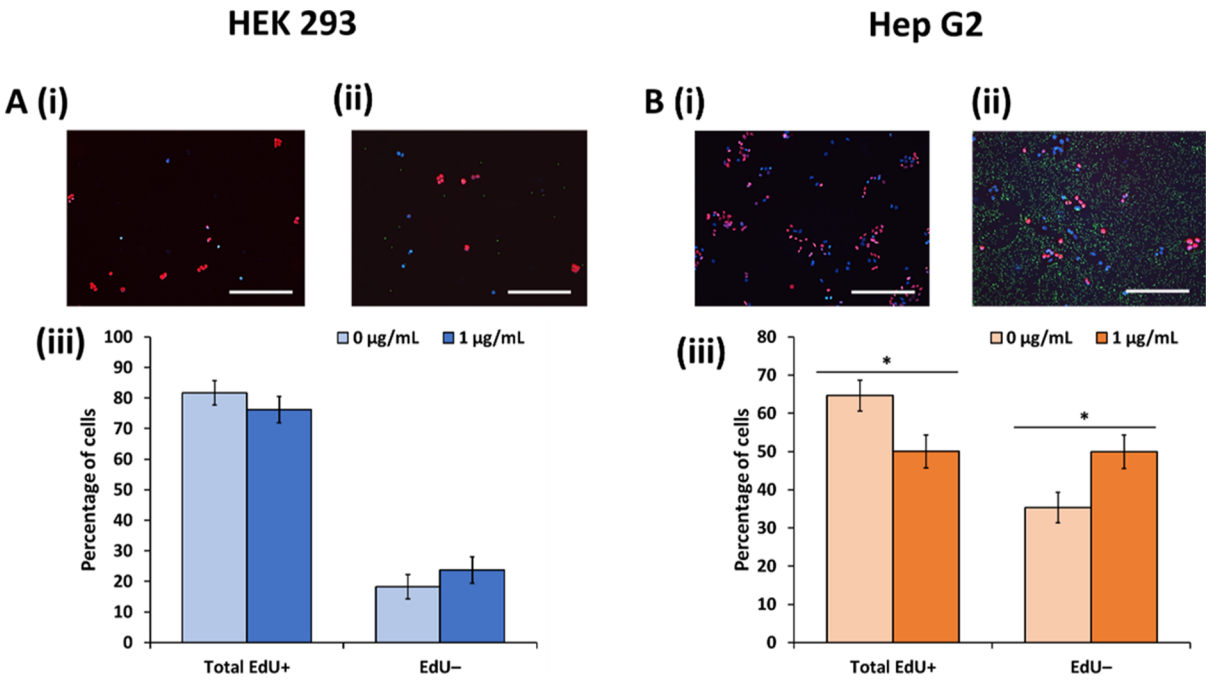

Figure 13. EdU labeling to characterize the cells in the S-phase. Both (A) HEK 293 and (B) Hep G2 cells were stained with 5-ethynyl-2′-deoxyuridine and counted for the total EdU+ (red and purple) and EdU− (blue) cells. Immunocytochemistry was carried out for the (i) untreated condition and (ii) 1 μg/mL PS-MP-treated. (iii) Cells in each image were counted and represented as a percentage. All cell images are shown in Supporting Information, Figures S17 and S18. Student's *t*-test was carried out to determine the significant. *: *p*-value < 0.05.

On the other hand, in Hep G2, 5 μg/mL induced the highest levels of ROS at all time points (Figure 11). The treatment of PS-MP at 100 μg/mL generated the least relative level of ROS and started to be comparable to 50 μg/mL after 12 h (Figure 11). Hydrogen peroxide treatment was used as the positive control, and cells with no MP treatment and no ROS label were used as the negative control (Supporting Information, Figure S15).

Microplastic Treatment Lowers Glycolytic Activity and Decreases the Gene Expression of ROS Cleanup Markers. Relative gene expression for antioxidant markers superoxide dismutase 2 (*SOD2*) and catalase (*CAT*) and the glycolysis marker glyceraldehyde 3-phosphate dehydrogenase (*GAPDH*) was measured in unexposed and exposed HEK 293 and Hep G2 cells using quantitative real-time polymerase chain reaction (qRT-PCR) at 24 and 72 h time points. Unexposed cells had no microplastic treatment, and exposed cells were treated with 5 and 100 μg/mL PS-MPs. At 24 and 72 h, the MP treatment at 5 and 100 μg/mL decreased the gene expression of *SOD2* and *CAT* by at least 50% when compared with the untreated HEK 293 cells at 24 and 72 h. The MP treatment also decreased the *GAPDH* marker, but it was more significant at 72 h (Figure 12A). Similarly, the MP treatment at 5 and 100 μg/mL also decreased *GAPDH*, *SOD2*, and *CAT* makers in Hep G2 cells. However, the high concentration 100 μg/mL showed lower average relative gene expression for all markers at both time points except CAT at 24 h (Figure 12B). Overall, the HEK 293 cells showed a decrease in expression of *SOD2* and *CAT* at both 24 h and even further at 72 h at 5 and 100 μg/mL MP exposure which indicates a lower expression of ROS cleanup markers. Additionally, *GAPDH* showed a decrease in expression at 24 and 72 h after MP exposure which suggests lower glycolytic activity in cells.

On the other hand, exposing Hep G2 cells to MP over time (24 vs 72 h) decreased the gene expression of *SOD2* and *CAT*. For the 72 h treatment, there was a decrease in *GAPDH* even at low 5 μg/mL concentration of MP treatment. Only a high concentration of 100 μg/mL of MP decreased the *SOD2* and *CAT* in the 72 h culture [Figure 12C(ii)]. Therefore, the Hep G2 cells showed a decrease in expression of *SOD2* and *CAT* at both 24 and 72 h at 5 and 50 μg/mL MP exposure which indicates a lower expression of ROS cleanup markers. Also, *GAPDH* showed a decrease in expression at 24 h and even more at 72 h after MP exposure, suggesting lower glycolytic activity in long-term exposure.

Cell Proliferation Detection by EdU in HEK 293 and Hep G2 Cells. As a thymidine analogue, 5-ethynyl-2′-deoxyuridine (EdU) can be used to detect the cells in the S phase in which the cell's DNA is being synthesized.[77] Using the Click-it reaction, a red fluorescent azide dye attaches itself to the EdU alkyne group in the newly synthesized DNA. Cells that have synthesized DNA have a bright red fluorescent signal, cells that are in the process of DNA synthesis are purple, and cells that are not in the process of DNA synthesis are blue (due to the nuclear stain Hoescht). Using this assay and taking fluorescent images, the red, purple, and blue cells were counted in each image and we were able to determine how many cells (a) synthesized DNA, (b) were in the process of DNA synthesis, and (c) were not in the process of DNA synthesis. The EdU label was added to cells, 1 μm green microplastics were added to appropriate wells, and cells were incubated for 24 h. For the graphs [shown in A(iii) and B(iii)] of Figure 13 at the 24 h time point, EdU-positive and partially EdU-positive cells were counted and combined to give the total relative percentage of EdU-positive cells. HEK 293 and Hep G2 unexposed cells had more total EdU-positive cells than microplastic-exposed cells. Furthermore, statistics shown in the graphs below show that PS-MP treatment of Hep G2 significantly decreased the cell percentage in the S-phase as compared to HEK 293 cells which did not show significant

https://doi.org/10.1021/acsomega.2c03453
ACS Omega 2022, 7, 34136−34153

changes between the percentage of cells in the S phase and not in the S phase. All EdU images are shown in Supporting Information, Figures S17 and S18.

DISCUSSION

In this work, we have identified 1 μm polystyrene microplastics inside HEK 293 kidney and Hep G2 liver cells in three different ways. We first noticed the internalization of PS-MPs in live cells by phase-contrast images at times points up to 72 h (Figures 1 and 2). Then, we used confocal microscopy to show the internalization of 1 μm, green-fluorescent, PS-MPs in both cell lines (Figures 4 and 5 and Supporting Information, Figures S1−S8). Finally, we used flow cytometry to confirm the percentage of HEK 293 kidney and Hep G2 liver cells positive for internalized microplastics (Figure 7 and Supporting Information Figures S9−S12). The observations of this study are consistent with our previous work using A459 human lung cells.[62]

Our work modeled what would happen when human kidney and liver cells are exposed to 1 μm polystyrene microspheres using environmentally relevant concentrations.[78] In this work, we uncovered several significant and noteworthy findings. First, we noted a decline in the net metabolic activity for HEK 293 and Hep G2 cells exposed to microplastics (Figure 8). At 24 h, exposed HEK 293 cultures experienced an initial 41% decline in the net metabolic activity, and by 72 h, the decline had reached 61%. The metabolic activity for exposed HEK 293 cultures was significantly lower than the unexposed cultures. This change signified the adverse impacts of microplastics on these cells within a 24−72 h time frame. Unlike HEK 293 exposed cultures that continued to see a decline in the net metabolic activity over time, Hep G2 exposed cultures experienced an initial decline at 24 h. This decline remained constant throughout the subsequent time points of 48 and 72 h. A noted metabolic decline in cellular activity was observed for both HEK 293 and Hep G2 exposed cultures. The metabolic effect was more severe for HEK 293 exposed cultures than Hep G2 exposed cultures, suggesting that microplastics can affect cells differently.

Second, we noted a difference in the proliferative rate for HEK 293 kidney and Hep G2 liver exposed cultures (Figure 6). 1 μm polystyrene microplastics did cause a slowdown in cell proliferation in both cell lines. For HEK 293 kidney cells, unexposed cultures grew as expected. At 24 h, both unexposed and exposed cultures grew similarly. However, by 48 h, exposed cultures began to show a significant decline in cell proliferation. By 72 h, the final cell number for exposed HEK 293 cells was less than 10% of its unexposed counterparts. Hep G2 unexposed cells also grew normally and exhibited a normal growth rate. Like HEK 293 exposed cultures, Hep G2 exposed cultures began to show a significant decline by 48 h in cell proliferation. By 72 h, the final cell number for exposed Hep G2 cells was less than 40% of its unexposed counterparts. HEK 293 kidney and Hep G2 liver cell cultures experienced significant declines in cellular proliferation rates due to microplastic exposure. This marked a change and a decline in the net metabolic activity, which is an indicator of alterations occurring within the cells. Although viability remained high for both cell lines exposed to microplastics, it is possible that prolonged exposure could lead to delayed effects. Our results were consistent with a previous investigation of the effect of MP on HEK 293 cells. At microplastic concentrations less than 25 μg/mL, the cell viability was more than 85%.[79]

Additionally, EdU results support our proliferation studies. Both HEK 293 and Hep G2 unexposed cells had more total EdU positive cells than microplastic-exposed cells at 24 h (Figure 13). Looking at the cell proliferation graphs shown in Figure 6, it is clear that these results correlate with the information at 24 h, where the unexposed cells are proliferating more than the MP-exposed cells in both cell lines. Overall, we were able to show that proliferation results are consistent in both our cell proliferation and EdU studies.

Third, we found a marked change in cellular morphology of HEK 293 kidney and Hep G2 liver cells exposed to 1 μm polystyrene microplastics Figures 1 and 2. HEK 293 kidney cells normally grow in clusters with long fingerlike projections protruding from cells. At 24 h, no significant differences were observed between unexposed and exposed cultures. By 48 h, cells exposed to microplastics began to show blebbing in some clusters of cells, and more single cells were observed. However, by 72 h, for exposed cells, severe blebbing was noted in many clusters, more singlets were observed, and cells in clusters did not show long, fingerlike projections trying to connect to nearby neighbors like in unexposed cells. The blebbing effect in our work is similar to results in HEK 293 kidney cells that were permeabilized with streptolysin O.[80] Similar to HEK 293 cells, exposed Hep G2 cells at 24 h showed little difference compared to their unexposed cells. At 48 h, Hep G2 exposed cells began to decluster, and more singlet cells were observed. By 72 h, there was severe declustering of cells, cells no longer formed tightly packed groups, and cells were becoming more spread-like in form. The declustering effect in our work is similar to results in Hep G2 cells exposed to gold nanoparticles.[81] These results showed that microplastics induced morphological changes in HEK 293 kidney and Hep G2 liver cells.

Fourth, we noted an increase in cellular stress in the HEK 293 and Hep G2 cell lines using an ROS live cell assay. Our most significant findings of this study revealed that HEK 293 and Hep G2 cells exposed to polystyrene microplastics had a steady increase in ROS levels over time for each concentration. This trend is shown in Supporting Information, Figures S13 and S15. We also show how the concentration of PS-MPs affects ROS levels at each time point (Figures 10 and 11). By 2 h, the HEK 293 50 μg/mL exposed cells had the highest ROS levels and maintained the highest throughout the observed time points of 4, 6, 12, and 24 h (Figure 10). However, for Hep G2 cells, results show that the lowest concentration of 5 μg/mL produces the greatest ROS response in liver cells at all time points compared with the higher concentrations, 50 and 100 μg/mL (Figure 11). These results show that depending on the cell line, concentration, and time, 1 μm polystyrene microplastics will induce a different cellular stress response.

Additionally, RT-PCR analysis was carried out to observe the relative gene expression of antioxidant markers *superoxide dismutase 2* (*SOD2*) and *catalase* (*CAT*) and the glycolysis marker *glyceraldehyde 3-phosphate dehydrogenase* (*GAPDH*) at time points of 24 and 72 h in HEK 293 and Hep G2 cells. HEK 293 cells showed lower expression of *SOD2* and *CAT* for 5 and 100 μg/mL exposed cells at 24 and 72 h, while Hep G2 cells showed lower expression of *SOD2* and *CAT* for 5 and 50 μg/mL exposed cells at 24 and 72 h (Figure 12). Furthermore, *GAPDH* showed a decrease in expression at 24 and 72 h after MP exposure. These results indicate that PS-MPs lower

https://doi.org/10.1021/acsomega.2c03453
ACS Omega 2022, 7, 34136−34153

glycolytic activity and inhibit the ability of antioxidant enzymes to cleanse ROS in both cell lines. These findings are very significant in that 1 μm PS-MPs cause the cells to not only be under severe stress but also limit the cell's ability to reduce or rid itself of harmful ROS. These results combined demonstrate the remarkable ability of PS-MPs to cause extenuating damage to cells that could lead to long-term adverse effects.

In addition to cellular stress changes, we observed that both HEK 293 kidney and Hep G2 liver cells internalized 1 μm polystyrene microspheres without adding functional groups to aid in internalization. Both cell lines internalized many particles, and single-cell phase-contrast images showed particles accumulating around the nuclei in clusters and in a ring-like pattern (Figure 3). Moreover, confocal fluorescent images at 72 h showed internalization of 1 μm green-fluorescent particles (Figures 4 and 5). Finally, flow cytometry experiments quantified the percentage of cells that internalized green-fluorescent microplastic particles. Both cell lines exposed to a lower concentration of 5 μg/mL showed a time-dependent increase in cells taking up PS-MP particles over time, and cells exposed to a higher concentration of 100 μg/mL took up more PS-MP particles, showing a similar amount of PS-MP uptake at 48 and 72 h (Figure 7).

As early as 24 h, the effects of microplastic exposure were initiated, although the full processes took much longer. By 48 h, distinct morphological differences were observed in exposed cells, and by 72 h, morphological changes were so severe that exposed cells were completely different from unexposed cells. Additionally, there was a noticeable net metabolic decline in exposed cells for all time points tested compared to unexposed cells. Furthermore, cellular proliferation was significantly inhibited for later time points tested, making it impossible to catch back up with their unexposed counterparts. Each experiment showed that microplastics significantly impacted cellular morphology, metabolism, proliferation, cellular stress, and internalization in HEK 293 kidney and Hep G2 liver cells.

The effect of MP may be due to both the nonspecific effects (size) and/or the specific effect (plastic material). In the Schirinzi et al. study, Hela cells exposed to 10 μm polystyrene microplastics caused significant ROS effects, but Hela cells exposed to 3−16 μm polyethylene microplastics caused no ROS effects.[82] In our previous work, we noted that the size caused a significant difference in effect, although both sizes tested were polystyrene microplastics and the studies were conducted in the same A549 human lung cell line.[62] Such studies demonstrate that both the type of material (plastic) and size affect cell lines differently. It should also be noted that many studies choose sizes that are not found in our natural environment. For our previous study, we chose 1 and 10 μm MPs because these were normal sizes detected in the air.[62] For this study, we chose the 1 μm size because it is commonly found in human foods and beverages that are highly consumed.[32,60,61] In this way, we are studying the effects of plastic particles that our body has more than likely been exposed to. In the future, glass beads and other materials will be used as control conditions to further evaluate the effect of microplastics on both HEK 293 and Hep G2 cells.

Although microplastics may not have immediate effects, they could cause delayed effects. A recent study published found polystyrene microplastics in human blood samples.[83] Once in the blood, it is possible for microplastics to translocate to different organs in the body, such as the kidney or liver. The liver, which has a specific role in filtering toxins from the blood, is one of the first potential deposit sites for microplastics. The kidney, whose primary function is to rid the body of wastes, is another important organ for accumulation of microplastics. Microplastics that evade filtration by the liver and kidneys can collect in these organs and possibly cause severe health issues over time. In vivo studies in mice have shown the adverse effects of microplastics on both the liver and kidneys. Microplastic accumulation in the liver of mice led to adverse effects such as oxidative stress, inflammation, altered energy metabolism, and damage to the liver.[84,85] Moreover, in another study, accumulation of microplastics in the kidney of mice led to histopathological damage, increased levels of endoplasmic reticulum stress markers, inflammatory markers, and nephrotoxicity.[86] Finally, our work shows that inhibition in cell proliferation, altered metabolism, cellular stress, and morphological changes all together can cause various alterations in cellular activity and affect the overall function of the cells, preventing cells from performing their normal functions. This may lead to long-term complications such as abnormal development of organs, tissue degeneration, and even organ failure. Thus, long-term ingestion of microplastics could cause chronic health conditions mediated by altered cellular functions, making disease susceptibility more likely.

■ ASSOCIATED CONTENT

Supporting Information

The Supporting Information is available free of charge at https://pubs.acs.org/doi/10.1021/acsomega.2c03453.

Characteristics of 1 μm polystyrene microplastic spheres (PS-MPs) from material data sheet; primer pairs for the markers of interest; confocal HEK 293 kidney cell images taken at 72 h; confocal HEK 293 kidney cell images taken at 72 h; confocal HEK 293 kidney cell images taken at 72 h; confocal microscopy images showing the separate fluorescent channels of HEK 293 kidney cells unexposed and exposed to 1 μm green-fluorescent PS-MPs; confocal Hep G2 liver cell images taken at 72 h; confocal Hep G2 liver cell images taken at 72 h; confocal Hep G2 liver cell images taken at 72 h; confocal microscopy images showing the separate fluorescent channels of Hep G2 liver cells unexposed and exposed cells to 1 μm green-fluorescent PS-MPs; dot plot of HEK 293 kidney cell flow cytometry gating population that internalized 1 μm polystyrene microplastics at 24, 48, and 72 h time points; flow cytometry histograms of the percentage of HEK 293 kidney cells that internalized 1 μm polystyrene microplastics at 24, 48, and 72 h time points; dot plot of Hep G2 liver cell flow cytometry gating population that internalized 1 μm polystyrene microplastics at 24, 48, and 72 h time points; flow cytometry histograms of the percentage of Hep G2 liver cells that internalized 1 μm polystyrene microplastics at 24, 48, and 72 h time points; relative fluorescence units of ROS induced by PS-MPs at different time points in HEK 293 kidney cells; positive and negative control treatment for ROS assay for HEK 293 kidney cells at 0, 2, 4, 6, 12, and 24 h time points; relative fluorescence units of ROS induced by PS-MPs at different time points in Hep G2 liver cells; positive and negative control treatment for ROS assay for Hep G2 liver cells at 0, 2, 4, 6, 12, and 24 h time points; EdU

https://doi.org/10.1021/acsomega.2c03453
ACS Omega 2022, 7, 34136−34153

staining images for HEK 293 kidney cells; and EdU staining images for Hep G2 liver cells (PDF)

AUTHOR INFORMATION

Corresponding Author

Qing-Xiang Amy Sang − *Department of Chemistry and Biochemistry, Florida State University, Tallahassee, Florida 32306, United States; Institute of Molecular Biophysics, Florida State University, Tallahassee, Florida 32306, United States;* orcid.org/0000-0001-8828-0569; Email: qxsang@chem.fsu.edu

Authors

Kerestin E. Goodman − *Department of Chemistry and Biochemistry, Florida State University, Tallahassee, Florida 32306, United States*

Timothy Hua − *Department of Chemistry and Biochemistry, Florida State University, Tallahassee, Florida 32306, United States*

Complete contact information is available at: https://pubs.acs.org/10.1021/acsomega.2c03453

Notes

The authors declare no competing financial interest.

ACKNOWLEDGMENTS

The authors would like to thank Dr. James Fadool for training on confocal microscopy at the FSU Biological Science Imaging Resource facility, Dr. Joan Hare for discussions and suggestions on some aspects of the experiments, Dr. Michael Roper laboratory for the Hep G2 cells, Dr. Gwimoon Seo for use of the Protein Expression Facility at the FSU Institute of Molecular Biophysics, and Beth Alexander's assistance with the flow cytometry experiment at the FSU Flow Cytometry Laboratory at College of Medicine. We would also like to thank Dr. Brian Washburn for his assistance with RT-PCR at the FSU Molecular Cloning Facility at the Department of Biological Science. This research has also used resources provided by the Materials Characterization Laboratory at the FSU Department of Chemistry and Biochemistry (FSU075000MAC), under the supervision of Dr. Raaj Vellore Winfred. This work was supported by the Council on Research & Creativity (CRC) planning grant from the Florida State University, Pfeiffer Professorship for Cancer Research in Chemistry and Biochemistry from the College of Arts & Sciences, and an Endowed Chair Professorship in Cancer Research from anonymous donors (to QXS), as well as Joseph M. Schor Graduate Fellowships in Biochemistry from FSU (to K.E.G. and T.H.) and McKnight Dissertation Fellowship from Florida Education Fund (to K.E.G.).

REFERENCES

(1) Horton, A. A.; Dixon, S. J. Microplastics: An Introduction to Environmental Transport Processes. *WIREs Water* **2018**, *5*, No. e1268.

(2) Zhang, Y.; Kang, S.; Allen, S.; Allen, D.; Gao, T.; Sillanpää, M. Atmospheric Microplastics: A Review on Current Status and Perspectives. *Earth-Sci. Rev.* **2020**, *203*, 103118.

(3) Wang, C.; Zhao, J.; Xing, B. Environmental Source, Fate, and Toxicity of Microplastics. *J. Hazard. Mater.* **2021**, *407*, 124357.

(4) Chen, Y.; Awasthi, A. K.; Wei, F.; Tan, Q.; Li, J. Single-Use Plastics: Production, Usage, Disposal, and Adverse Impacts. *Sci. Total Environ.* **2021**, *752*, 141772.

(5) Plasctic Europe—Association of Plastics Manufactures. Plastics—The Facts 2020. *Plast Europe*, 2020; pp 1−64.

(6) EPA. *Advancing Sustainable Materials Management*; U.S. Environmental Protection Agency, 2020. No 184. December.

(7) Dissanayake, P. D.; Kim, S.; Sarkar, B.; Oleszczuk, P.; Sang, M. K.; Haque, M. N.; Ahn, J. H.; Bank, M. S.; Ok, Y. S. Effects of Microplastics on the Terrestrial Environment: A Critical Review. *Environ. Res.* **2022**, *209*, 112734.

(8) Xiang, Y.; Jiang, L.; Zhou, Y.; Luo, Z.; Zhi, D.; Yang, J.; Lam, S. S. Microplastics and Environmental Pollutants: Key Interaction and Toxicology in Aquatic and Soil Environments. *J. Hazard. Mater.* **2022**, *422*, 126843.

(9) Chen, G.; Feng, Q.; Wang, J. Mini-Review of Microplastics in the Atmosphere and Their Risks to Humans. *Sci. Total Environ.* **2020**, *703*, 135504.

(10) Evangeliou, N.; Grythe, H.; Klimont, Z.; Heyes, C.; Eckhardt, S.; Lopez-Aparicio, S.; Stohl, A. Atmospheric Transport Is a Major Pathway of Microplastics to Remote Regions. *Nat. Commun.* **2020**, *11*, 3381.

(11) Luo, W.; Su, L.; Craig, N.; Du, F.; Wu, C.; Shi, H. Comparison of Microplastic Pollution in Different Water Bodies from Urban Creeks to Coastal Waters. *Environ. Pollut.* **2019**, *246*, 174−182.

(12) Abbasi, S.; Keshavarzi, B.; Moore, F.; Turner, A.; Kelly, F.; Dominguez, A.; Jaafarzadeh, N. Distribution and Potential Health Impacts of Microplastics and Microrubbers in Air and Street Dusts from Asaluyeh County, Iran. *Environ. Pollut.* **2019**, *244*, 153−164.

(13) Shim, W. J.; Thomposon, R. C. Microplastics in the Ocean. *Arch. Environ. Contam. Toxicol.* **2015**, *69*, 265−268.

(14) Zhang, Y.; Gao, T.; Kang, S.; Allen, S.; Luo, X.; Allen, D. Microplastics in Glaciers of the Tibetan Plateau: Evidence for the Long-Range Transport of Microplastics. *Sci. Total Environ.* **2021**, *758*, 143634.

(15) Barasarathi, J. MICROPLASTIC ABUNDANCE IN SELECTED MANGROVE FOREST IN MALAYSIA. *Proceeding of the ASEAN Conference on Science and Technology*; ASEAN, 2014.

(16) Patchaiyappan, A.; Dowarah, K.; Zaki Ahmed, S.; Prabakaran, M.; Jayakumar, S.; Thirunavukkarasu, C.; Devipriya, S. Prevalence and Characteristics of Microplastics Present in the Street Dust Collected from Chennai Metropolitan City, India. *Chemosphere* **2021**, *269*, 128757.

(17) Bergmann, M.; Mützel, S.; Primpke, S.; Tekman, M.; Trachsel, J.; Gerdts, G. White and Wonderful? Microplastics Prevail in Snow from the Alps to the Arctic. *Sci. Adv.* **2019**, *5*, No. eaax1157.

(18) De-la-Torre, G. E. Microplastics: an emerging threat to food security and human health. *J. Food Sci. Technol.* **2020**, *57*, 1601−1608.

(19) Cox, K. D.; Covernton, G. A.; Davies, H. L.; Dower, J. F.; Juanes, F.; Dudas, S. E. Human Consumption of Microplastics. *Environ. Sci. Technol.* **2019**, *53*, 7068−7074.

(20) Liebezeit, G.; Liebezeit, E. Non-pollen particulates in honey and sugar. *Non-Pollen Particulates in Honey and Sugar* **2013**, *30*, 2136−2140.

(21) Lee, H.; Kunz, A.; Shim, W. J.; Walther, B. A. Microplastic Contamination of Table Salts from Taiwan, Including a Global Review. *Sci. Rep.* **2019**, *9*, 10145.

(22) Kim, J.-S.; Lee, H.-J.; Kim, S.-K.; Kim, H.-J. Global Pattern of Microplastics (MPs) in Commercial Food-Grade Salts: Sea Salt as an Indicator of Seawater MP Pollution. *Environ. Sci. Technol.* **2018**, *52*, 12819−12828.

(23) Hernandez, L.; Xu, E.; Larsson, H.; Tahara, R.; Maisuria, V.; Tufenkji, N. Plastic Teabags Release Billions of Microparticles and Nanoparticles into Tea. *Environ. Sci. Technol.* **2019**, *53*, 12300−12310.

(24) Liebezeit, G.; Liebezeit, E. Synthetic Particles as Contaminants in German Beers. *Food Addit. Contam., Part A: Chem., Anal., Control, Exposure Risk Assess.* **2014**, *31*, 1574−1578.

(25) Diaz-Basantes, M. F.; Conesa, J. A.; Fullana, A. Microplastics in Honey, Beer, Milk and Refreshments in Ecuador as Emerging Contaminants. *Sustainability* **2020**, *12*, 5514.

(26) Pivokonsky, M.; Cermakova, L.; Novotna, K.; Peer, P.; Cajthaml, T.; Janda, V. Occurrence of Microplastics in Raw and Treated Drinking Water. *Sci. Total Environ.* **2018**, *643*, 1644−1651.
(27) Wang, Z.; Lin, T.; Chen, W. Occurrence and Removal of Microplastics in an Advanced Drinking Water Treatment Plant (ADWTP). *Sci. Total Environ.* **2020**, *700*, 134520.
(28) Kosuth, M.; Mason, S. A.; Wattenberg, E. V. Anthropogenic Contamination of Tap Water, Beer, and Sea Salt. *PLoS One* **2018**, *13*, No. e0194970.
(29) Oßmann, B. E.; Sarau, G.; Holtmannspötter, H.; Pischetsrieder, M.; Christiansen, S. H.; Dicke, W. Small-Sized Microplastics and Pigmented Particles in Bottled Mineral Water. *Water Res.* **2018**, *141*, 307−316.
(30) Zuccarello, P.; Ferrante, M.; Cristaldi, A.; Copat, C.; Grasso, A.; Sangregorio, D.; Fiore, M.; Oliveri Conti, G. Exposure to Microplastics (<10 μm) Associated to Plastic Bottles Mineral Water Consumption: The First Quantitative Study. *Water Res.* **2019**, *157*, 365−371.
(31) Mason, S. A.; Welch, V. G.; Neratko, J. Synthetic Polymer Contamination in Bottled Water. *Front. Chem.* **2018**, *6*, 407.
(32) Zhang, Q.; Xu, E. G.; Li, J.; Chen, Q.; Ma, L.; Zeng, E. Y.; Shi, H. A Review of Microplastics in Table Salt, Drinking Water, and Air: Direct Human Exposure. *Environ. Sci. Technol.* **2020**, *54*, 3740−3751.
(33) Fao. *Microplastics in Fisheries and Aquaculture Status of Knowledge on Their Occurrence and Implications for Aquatic Organisms and Food Safety*, 2017.
(34) Smith, M.; Love, D.; Rochman, C.; Neff, R. Microplastics in Seafood and the Implications for Human Health. *Curr. Environ. Health Rep.* **2018**, *5*, 375.
(35) Guillen, J.; Natale, F.; Carvalho, N.; Casey, J.; Hofherr, J.; Druon, J. N.; Fiore, G.; Gibin, M.; Zanzi, A.; Martinsohn, J. T. Global Seafood Consumption Footprint. *Ambio* **2019**, *48*, 111−122.
(36) Pritzker, P.; Sullivan, K.; Sobeck, E. *Fisheries of the United States 2015*; National Oceanic and Atmospheric Administration: Silver Spring, MD, 2016. https://www.fisheries.noaa.gov/feature-story/fisheries-united-states-2015.
(37) Ross, W.; Jacobs, N.; Oliver, C. *Fisheries of the United States 2018*; National Oceanic and Atmospheric Administration: Silver Spring, MD, 2020. https://www.fisheries.noaa.gov/national/commercial-fishing/fisheries-united-states-2018.
(38) Raimondo, G.; Friedman, B.; Doremus, P. *Fisheries of the United States 2019*; National Oceanic and Atmospheric Administration: Silver Spring, MD, 2021. https://www.fisheries.noaa.gov/resource/document/fisheries-united-states-2019.
(39) Curren, E.; Leaw, C.; Lim, P.; Leong, S. Evidence of Marine Microplastics in Commercially Harvested Seafood. *Front. Bioeng. Biotechnol.* **2020**, *8*, 1390.
(40) Gurjar, U.; Xavier, M.; Nayak, B.; Ramteke, K.; Deshmukhe, G.; Jaiswar, A.; Shukla, S. Microplastics in Shrimps: A Study from the Trawling Grounds of North Eastern Part of Arabian Sea. *Environ. Sci. Pollut. Res.* **2021**, *28*, 48494−48504.
(41) Imasha, I.; Babel, S. Microplastics Contamination in Commercial Green Mussels from Selected Wet Markets in Thailand. *Arch. Environ. Contam. Toxicol.* **2021**, *81*, 449−459.
(42) Li, J.; Qu, X.; Su, L.; Zhang, W.; Yang, D.; Kolandhasamy, P.; Li, D.; Shi, H. Microplastics in Mussels along the Coastal Waters of China. *Environ. Pollut.* **2016**, *214*, 177−184.
(43) Li, J.; Green, C.; Reynolds, A.; Shi, H.; Rotchell, J. M. Microplastics in Mussels Sampled from Coastal Waters and Supermarkets in the United Kingdom. *Environ. Pollut.* **2018**, *241*, 35−44.
(44) Wootton, N.; Ferreira, M.; Reis-Santos, P.; Gillanders, B. M. A Comparison of Microplastic in Fish From Australia and Fiji. *Front. Mar. Sci.* **2021**, *8*, 690991.
(45) Xu, K.; Zhang, Y.; Huang, Y.; Wang, J. Toxicological Effects of Microplastics and Phenanthrene to Zebrafish (Danio Rerio). *Sci. Total Environ.* **2021**, *757*, 143730.
(46) Zitouni, N.; Bousserrhine, N.; Missawi, O.; Boughattas, I.; Chèvre, N.; Santos, R.; Belbekhouche, S.; Alphonse, V.; Tisserand, F.; Balmassiere, L.; Dos Santos, S. P.; Mokni, M.; Guerbej, H.; Banni, M. Uptake, Tissue Distribution and Toxicological Effects of Environmental Microplastics in Early Juvenile Fish Dicentrarchus Labrax. *J. Hazard. Mater.* **2021**, *403*, 124055.
(47) Egbeocha, C.; Malek, S.; Emenike, C.; Milow, P. Feasting on Microplastics: Ingestion by and Effects on Marine Organisms. *Aquat. Biol.* **2018**, *27*, 93−106.
(48) Bai, Z.; Wang, N.; Wang, M. Effects of Microplastics on Marine Copepods. *Ecotoxicol. Environ. Saf.* **2021**, *217*, 112243.
(49) Teng, J.; Zhao, J.; Zhu, X.; Shan, E.; Zhang, C.; Zhang, W.; Wang, Q. Toxic Effects of Exposure to Microplastics with Environmentally Relevant Shapes and Concentrations: Accumulation, Energy Metabolism and Tissue Damage in Oyster Crassostrea Gigas. *Environ. Pollut.* **2021**, *269*, 116169.
(50) Avio, C. G.; Gorbi, S.; Milan, M.; Benedetti, M.; Fattorini, D.; d'Errico, G.; Pauletto, M.; Bargelloni, L.; Regoli, F. Pollutants Bioavailability and Toxicological Risk from Microplastics to Marine Mussels. *Environ. Pollut.* **2015**, *198*, 211−222.
(51) Yin, L.; Chen, B.; Xia, B.; Shi, X.; Qu, K. Polystyrene Microplastics Alter the Behavior, Energy Reserve and Nutritional Composition of Marine Jacopever (Sebastes Schlegelii). *J. Hazard. Mater.* **2018**, *360*, 97−105.
(52) Yu, P.; Liu, Z.; Wu, D.; Chen, M.; Lv, W.; Zhao, Y. Accumulation of Polystyrene Microplastics in Juvenile Eriocheir Sinensis and Oxidative Stress Effects in the Liver. *Aquat. Toxicol.* **2018**, *200*, 28−36.
(53) Prata, J. C.; da Costa, J. P.; Duarte, A. C.; Rocha-Santos, T. Suspected Microplastics in Atlantic Horse Mackerel Fish (Trachurus Trachurus) Captured in Portugal. *Mar. Pollut. Bull.* **2022**, *174*, 113249.
(54) Sui, M.; Lu, Y.; Wang, Q.; Hu, L.; Huang, X.; Liu, X. Distribution Patterns of Microplastics in Various Tissues of the Zhikong Scallop (Chlamys Farreri) and in the Surrounding Culture Seawater. *Mar. Pollut. Bull.* **2020**, *160*, 111595.
(55) Wu, B.; Wu, X.; Liu, S.; Wang, Z.; Chen, L. Size-Dependent Effects of Polystyrene Microplastics on Cytotoxicity and Efflux Pump Inhibition in Human Caco-2 cells. *Chemosphere* **2019**, *221*, 333−341.
(56) Wu, W.; Wu, W.; Tian, T.; Qiu, Q.; Li, L. Effects of polystyrene microbeads on cytotoxicity and transcriptomic profiles in human Caco-2 cells. *Environ. Toxicol.* **2020**, *35*, 495.
(57) Visalli, G.; Facciolà, A.; Pruiti Ciarello, M. P.; De Marco, G. D.; Maisano, M.; Di Pietro, A. D. Acute and Sub-Chronic Effects of Microplastics (3 and 10 μm) on the Human Intestinal Cells HT-29. *Int. J. Environ. Res. Publ. Health* **2021**, *18*, 5833.
(58) Wang, Y.-L.; Lee, Y.-H.; Hsu, Y.-H.; Chiu, I.-J.; Huang, C. C.-Y.; Huang, C.-C.; Chia, Z.-C.; Lee, C.-P.; Lin, Y.-F.; Chiu, H.-W. The Kidney-Related Effects of Polystyrene Microplastics on Human Kidney Proximal Tubular Epithelial Cells HK-2 and Male C57BL/6 Mice. *Environ. Health Perspect.* **2021**, *129*, 057003.
(59) Cheng, W.; Li, X.; Zhou, Y.; Yu, H.; Xie, Y.; Guo, H.; Wang, H.; Li, Y.; Feng, Y.; Wang, Y. Polystyrene Microplastics Induce Hepatotoxicity and Disrupt Lipid Metabolism in the Liver Organoids. *Sci. Total Environ.* **2022**, *806*, 150328.
(60) Barboza, L. G. A.; Dick Vethaak, A.; Lavorante, B. R. B. O.; Lundebye, A. K.; Guilhermino, L. Marine Microplastic Debris: An Emerging Issue for Food Security, Food Safety and Human Health. *Mar. Pollut. Bull.* **2018**, *133*, 336−348.
(61) Kutralam-Muniasamy, G.; Pérez-Guevara, F.; Elizalde-Martínez, I.; Shruti, V. C. Branded milks - Are they immune from microplastics contamination? *Sci. Total Environ.* **2020**, *714*, 136823.
(62) Goodman, K.; Hare, J.; Khamis, Z.; Hua, T.; Sang, Q. A. Exposure of Human Lung Cells to Polystyrene Microplastics Significantly Retards Cell Proliferation and Triggers Morphological Changes. *Chem. Res. Toxicol.* **2021**, *34*, 1069.
(63) Song, J. A.; Choi, C. Y.; Park, H.-S. Exposure of Bay Scallop Argopecten Irradians to Micro-Polystyrene: Bioaccumulation and Toxicity. *Comp. Biochem. Physiol., Part C: Toxicol. Pharmacol.* **2020**, *236*, 108801.

https://doi.org/10.1021/acsomega.2c03453
ACS Omega 2022, 7, 34136−34153

(64) Ullah, R.; Tsui, M. T.-K.; Chen, H.; Chow, A.; Williams, C.; Ligaba-Osena, A. Microplastics Interaction with Terrestrial Plants and Their Impacts on Agriculture. *J. Environ. Qual.* **2021**, *50*, 1024−1041.
(65) Chen, Y.; Ling, Y.; Li, X.; Hu, J.; Cao, C.; He, D. Size-Dependent Cellular Internalization and Effects of Polystyrene Microplastics in Microalgae P. Helgolandica Var. Tsingtaoensis and S. Quadricauda. *J. Hazard. Mater.* **2020**, *399*, 123092.
(66) Shang, X.; Lu, J.; Feng, C.; Ying, Y.; He, Y.; Fang, S.; Lin, Y.; Dahlgren, R.; Ju, J. Microplastic (1 and 5 μm) exposure disturbs lifespan and intestine function in the nematode Caenorhabditis elegans. *Sci. Total Environ.* **2020**, *705*, 135837.
(67) Buskermolen, A. B.; Kurniawan, N. A.; Bouten, C. V. An automated quantitative analysis of cell, nucleus and focal adhesion morphology. *PLoS One* **2018**, *13*, No. e0195201.
(68) Celik, F. S.; Cora, T.; Yigin, A. K. Investigation of Genotoxic and Cytotoxic Effects of Acrylamide in HEK293 Cell Line. *J. Cancer Prev. Curr. Res.* **2018**, *9*, 260.
(69) Almeer, A.; Ali, A.; Alarifi, A.; Alkahtani, A.; Almansour, A. Green Platinum Nanoparticles Interaction With HEK293 Cells: Cellular Toxicity, Apoptosis, and Genetic Damage. *Dose-Response Publ. Int. Hormesis Soc.* **2018**, *16*, 1559325818807382.
(70) Cederbaum, A. I.; Wu, D.; Mari, M.; Bai, J. CYP2E1-dependent toxicity and oxidative stress in HepG2 cells,. *Free Radic. Biol. Med.* **2001**, *31*, 1539−1543.
(71) Moore, P. D.; Yedjou, C. G.; Tchounwou, P. B. Malathion-induced oxidative stress, cytotoxicity, and genotoxicity in human liver carcinoma (HepG2) cells. *Environ. Toxicol.* **2010**, *25*, 221−226.
(72) Sadeghi, L.; Tanwir, F.; Yousefi Babadi, V. In vitro toxicity of iron oxide nanoparticle: Oxidative damages on Hep G2 cells. *Exp. Toxicol. Pathol. Off. J. Ges. Toxikol. Pathol.* **2015**, *67*, 197−203.
(73) Ojo, A. F.; Peng, C.; Ng, J. C. Combined Effects and Toxicological Interactions of Perfluoroalkyl and Polyfluoroalkyl Substances Mixtures in Human Liver Cells (HepG2). *Environ. Pollut.* **2020**, *263*, 114182.
(74) Hua, T.; Kiran, S.; Li, Y.; Sang, Q.-X. A. Microplastics Exposure Affects Neural Development of Human Pluripotent Stem Cell-Derived Cortical Spheroids. *J. Hazard. Mater.* **2022**, *435*, 128884.
(75) Berridge, M. V.; Tan, A. S. Characterization of the Cellular Reduction of 3-(4,5-dimethylthiazol-2-yl)-2,5-diphenyltetrazolium bromide (MTT): Subcellular Localization, Substrate Dependence, and Involvement of Mitochondrial Electron Transport in MTT Reduction. *Arch. Biochem. Biophys.* **1993**, *303*, 474−482.
(76) Liu, Y.; Peterson, D. A.; Kimura, H.; Schubert, D. Mechanism of Cellular 3-(4,5-Dimethylthiazol-2-Yl)-2,5-Diphenyltetrazolium Bromide (MTT) Reduction. *J. Neurochem.* **1997**, *69*, 581−593.
(77) Zeng, C.; Pan, F.; Jones, L. A.; Lim, M. M.; Griffin, E. A.; Sheline, Y. I.; Mintun, M. A.; Holtzman, D. M.; Mach, R. H. Evaluation of 5-ethynyl-2′-deoxyuridine staining as a sensitive and reliable method for studying cell proliferation in the adult nervous system. *Brain Res.* **2010**, *1319*, 21−32.
(78) Danopoulos, E.; Twiddy, M.; West, R.; Rotchell, J. M. A Rapid Review and Meta-Regression Analyses of the Toxicological Impacts of Microplastic Exposure in Human Cells. *J. Hazard. Mater.* **2022**, *427*, 127861.
(79) Sivagami, M.; Selvambigai, M.; Devan, U.; Velangani, A. A. J.; Karmegam, N.; Biruntha, M.; Arun, A.; Kim, W.; Govarthanan, M.; Kumar, P. Extraction of Microplastics from Commonly Used Sea Salts in India and Their Toxicological Evaluation. *Chemosphere* **2021**, *263*, 128181.
(80) Babiychuk, E. B.; Monastyrskaya, K.; Potez, S.; Draeger, A. Blebbing Confers Resistance against Cell Lysis. *Cell Death Differ.* **2011**, *18*, 80−89.
(81) Al-Khedhairy, A. A.; Wahab, R. Size-Dependent Cytotoxic and Molecular Study of the Use of Gold Nanoparticles against Liver Cancer Cells. *Appl. Sci.* **2022**, *12*, 901.
(82) Schirinzi, G. F.; Pérez-Pomeda, I.; Sanchís, J.; Rossini, C.; Farré, M.; Barceló, D. Cytotoxic Effects of Commonly Used Nanomaterials and Microplastics on Cerebral and Epithelial Human Cells. *Environ. Res.* **2017**, *159*, 579−587.
(83) Leslie, H. A.; van Velzen, M. J. M.; Brandsma, S. H.; Vethaak, A. D.; Garcia-Vallejo, J. J.; Lamoree, M. H. Discovery and Quantification of Plastic Particle Pollution in Human Blood. *Environ. Int.* **2022**, *163*, 107199.
(84) Deng, Y.; Zhang, Y.; Lemos, B.; Ren, H. Tissue Accumulation of Microplastics in Mice and Biomarker Responses Suggest Widespread Health Risks of Exposure. *Sci. Rep.* **2017**, *7*, 46687.
(85) Mu, Y.; Sun, J.; Li, Z.; Zhang, W.; Liu, Z.; Li, C.; Peng, C.; Cui, G.; Shao, H.; Du, Z. Activation of Pyroptosis and Ferroptosis Is Involved in the Hepatotoxicity Induced by Polystyrene Microplastics in Mice. *Chemosphere* **2022**, *291*, 132944.
(86) Meng, X.; Zhang, J.; Wang, W.; Gonzalez-Gil, G.; Vrouwenvelder, J. S.; Li, Z. Effects of Nano- and Microplastics on Kidney: Physicochemical Properties, Bioaccumulation, Oxidative Stress and Immunoreaction. *Chemosphere* **2022**, *288*, 132631.

https://doi.org/10.1021/acsomega.2c03453
ACS Omega 2022, 7, 34136−34153